NOVEL MATERIALS FOR POWER SYSTEMS. PART II. INVESTIGATIONS OF PROTON SEMI-CONDUCTING GLASSES

C. A. Angell

Purdue University

Prepared for:

Advanced Research Projects Agency

15 July 1974

UNCLASSIFIED
Security Classification

AD 784448

DOCUMENT CONTROL DATA - R & D

(Security classification of title, body of abstract and indexing annotation must be entered when the overall report is classified)

1. ORIGINATING ACTIVITY (Corporate author) Purdue Research Foundation - School of Electrical Engineering	2a. REPORT SECURITY CLASSIFICATION 2b. GROUP

3. REPORT TITLE
Novel Materials for Power Systems
PART II - Investigations of Proton Semi-Conducting Glasses

4. DESCRIPTIVE NOTES (Type of report and inclusive dates)
Annual Technical Report 6/1/73-5/31/74

5. AUTHOR(S) (First name, middle initial, last name)
C. A. Angell

6. REPORT DATE July 15, 1974	7a. TOTAL NO. OF PAGES 54	7b. NO. OF REFS 23
8a. CONTRACT OR GRANT NO DAHC15-73-G11 b. PROJECT NO ARPA Order No. 2338 Code No. 3D10 c. d.	9a. ORIGINATOR'S REPORT NUMBER(S) 9b. OTHER REPORT NO(S) (Any other numbers that may be assigned this report)	

10. DISTRIBUTION STATEMENT
Distribution of this document is unlimited

11. SUPPLEMENTARY NOTES	12. SPONSORING MILITARY ACTIVITY Defense Advanced Research Projects Agency 1400 Wilson Blvd. Arlington, Virginia 22209

13. ABSTRACT

The work performed under this program can be subdivided into three areas: PART I - Schizophrenic Catalysts; PART II - PROTONIC Semi-Conductors; and PART III - Selective Emitters for Energy Conversion.

PART II - Protonic Semi-Conductors

The phenomenon of unusually large electrical conductivity in glasses formed by the cooling of certain aqueous solutions of strong protonic acids has been investigated with the object of 1) establishing that the origin of the excess conductivity lies in the high mobility of protons in the glassy structure, and 2) determining the states of protons responsible for the phenomenon and examining the relation of the operative conductance mechanism to that oxide glass with mobile alkali metal cations.

D.C. conductivity studies confirmed the protonic origin of the conductance, but showed also that the phenomenon was limited to glasses with relatively high glass transition temperatures. NMR and IR spectral studies showed that excess (acid) protons exchanged rapidly with water protons on the NMR time scale although two distinct proton environments are observed in the shorter time scale IR spectra. Conductivity relaxation studies were unable to find any basic differences in the electrical field response characteristics between the protonic conductors and the silicate glass ionic conductors.

UNCLASSIFIED

Security Classification

14 KEY WORDS	LINK A		LINK B		LINK C	
	ROLE	WT	ROLE	WT	ROLE	WT
Protonic Conduction						

DD FORM 1 NOV 68 1473 (BACK)
(PAGE 2)

12

Security Classification

Annual Technical Report
for the Period 6/1/73 - 5/31/74

Novel Materials for Power Systems

PART II

Investigations of Proton Semi-Conducting Glasses

Grant Number DAHC15-73-G11

Program Code No. 3D10

Grantee: Purdue Research Foundation

Project Director: R. J. Schwartz (317) 749-2467

Principal Investigator: C. A. Angell (317) 49-48331

Effective Date of Grant: 6/1/73

Grant Expiration Date: 5/31/74

Amount of Grant: $87,058.00

Sponsored by
Advanced Research Projects Agency
ARPA Order No. 2338

Investigations of Proton Semi-conducting Glasses

C. A. Angell

Summary

This work was executed with a view to determining the scientific interest in, and device potential of, the phenomenon of unusually large electrical conductivities exhibited by certain glasses prepared from strong acid solutions. It was conjectured that the anomalous conduction was due to this relatively unrestricted motion of protons (the heavy primary charged particles) through the glass structure. If true, this would provide an interesting comparison with the behavior of glasses on which electrons (the light primary charged particles) move relatively freely through the glass structure in the recently much-researched chalcogenide-type semi-conducting glasses. Since the latter glasses have proven to have important practical applications, the possibility existed that this might be true also of the former glasses. The primary objectives of this research, then, were to establish that the anomalous conductivity was indeed due to proton mobility, and then to discover, by the application of various research techniques, as much as possible about the proton migration mechanisms.

The project was therefore essentially an experimental one. The bulk of the work was to involve comparative electrical conductivity measurements by familiar bridge techniques on (i) various acid glasses and chemically similar non-acid glasses to prove the protonic origin of the acid glass conductance anomaly and (ii) selected acid glasses using wide frequency ranges to provide details on the actual conductance mechanism. The laboratory was already equipped to perform these measurements. Subsidiary studies, using NMR and infrared spectroscopy, were planned to determine as far as possible what

chemical species were important to the conductance properties i.e. what the chemical states of the conducting protons might be. A Varian A60 NMR Spectrometer was available in the Department, but the laboratory lacked a suitable instrument therefore became the primary capital equipment expenditure for this project. The instrument purchased was a Perkin Elmer Model No. 467.

The results may be stated simply. An initial series of measurements proved that the proton was indeed the mobile species, but that not all strong acids yielded high conducting glasses: an important additional requirement for high conductivity is that the absolute temperature be high relative to the activation energy for the primary proton jump process. This process appears to be essentially the same in all glasses studies.

Variable frequency studies established, perhaps surprisingly, that the overall kinetic character of the charge migration process is indistinguishable from that of fast alkali metal ion transport in common silicate glasses. The kinetic character is evidently determined by the laws of random diffusive motion, irrespective of the precise nature of the diffusing particle or the details of the primary migration.

Some evidence was obtained from IR spectroscopy combined with conductance data that very fast transport is only obtained when the water-to-proton ratio exceeds 2:1. Further investigation of this point would assist in understanding the basic migration mechanism. The research should be extended to involve studies of acid solutions with higher glass transition temperatures - e.g. as obtained with polymeric anions to see if very large but totally protonic can be observed. It is probable that such extensions of the present research would show a close relation between conductance in the glasses on this study, and the recently fabricated fluorinated hydrocarbon sulphouric acid resins developed by

DuPont for high efficiency electrolysis and fuel cell membranes. An outcome of continued research in this area would probably be an improvement in understanding of and hence technical performance of such membranes, which we believe will be important in the future as the nation moves toward a hydrogen economy.

Investigations of Proton Semi-Conducting Glasses

FINAL REPORT ON

Investigations of Proton Semi-Conducting Glasses

C. A. Angell

Department of Chemistry

I. Project Objectives

The object of this research was to explore the phenomenon of anomalously high electrical conductivities in the glassy state of certain solutions which contain protons loosely bound in the structure.[1,2]

In the first place it was to be demonstrated by systematic experiments, that the anomalous conductivity which had been observed was indeed due to the migration of protons through the vitreous quality lattice. The key experiments needed to establish the protonic origin of the excess conductance were deemed to be those in which the conductance was studied as a function of composition as the protons in an "anomalous" glass were systematically replaced by some charge-compensating ion.

In order to make results in different solutions comparable such measurements must be made at some corresponding temperature, such that the structural reorganization relaxation time, which determines the contribution which ordinary ions can make to the conduction process in these media, is the same. It has been convenient to choose the glass transition temperature to serve as this corresponding temperature since it is easily measured, and corresponds to a fixed structural relaxation time of about 1 sec. In order to eliminate the possibility of a direct temperature effect (about which more will be said below) the system chosen for this study was one in which the acid solution and its lithium substituted analogue have essentially the same glass transition temperatures. Such a system is the pseudo-binary $Li_2Cr_2O_7 \cdot 6H_2O + H_2Cr_2O_7 \cdot 6H_2O$.

The second objective of this research was to then characterize the mechanism by which protons migrate through the structure, to ascertain its relation to the mechanisms of conduction in high ionic conductivity oxide glasses, and to determine the types of sites between which such protons migrated.

To this end (i) an investigation of the frequency dependence of the electrical conductivity and the solution capacitance was to be performed so the complete electrical field response function of the medium could be determined, and

(ii) proton magnetic resonance and infrared spectral spectra were to be obtained so that the average state of magnetic deshielding of the protons, and the force fields in which different types of protons vibrate, could be determined.

The overall justification for this research might be regarded as (a) the interest in determining the extent to which, if at all, the migration of the heavy primary particle, the proton, in glass bears a resemblance to the migration of the light primary particle, the electron, in the now much studied semi-conducting chalcogenide type glass, and (b) to ascertain the potential usefulness of such proton conducting glasses in membrane functions such as in water electrolysis cells, where the ability to selectively pass protons might be of considerable value.

Electrical Relaxation

Since a major part of the recent work on this project deals with the study of the rather unfamiliar area of conductivity relaxation, we devote some space to this subject in this introductory section.

Dielectric relaxation is usually described in terms of the complex permitivity, ε^*, defined as

$$\varepsilon^* = \varepsilon' - i\varepsilon'' - i(\sigma/we_o) \tag{1}$$

where w is the angular frequency, ε' the dielectric constant, ε'' the dielectric loss, σ the specific conductivity, and e_o the permitivity of free space (8.854×10^{-14} fared cm^{-1}). The quantities ε' and σ are calculated from the experimentally measured resistance R and capacitance C via the equations

$$\varepsilon' = C/C_o \quad ; \quad \sigma = e_o/RC_o \tag{2}$$

where C_o is the vaccuum capacitance of the conductance cell.

Electrical relaxation which occurs by the diffusing of ions, rather than the rotation of dipoles, has been termed "conductivity relaxation"[3], and for two reasons is better treated in an "electric modulus" formalism rather than in the usual complex permitivitv formalism.[3] The electric modulus M^* is related to the complex permitivity by

$$M^* = M' + iM' = 1/\varepsilon^* \tag{3}$$

Conductivity relaxation in amorphous materials is generally discussed in terms of a distribution of relaxation times, $g(\tau_\sigma)$, and the expressions for M' and M'' are

$$M' = \left\langle \frac{(w\tau_\sigma)^2}{1 + (w\tau_\sigma)^2} \right\rangle \tag{4}$$

$$M'' = \left\langle \frac{(w\tau_\sigma)}{1 + (w\tau_\sigma)^2} \right\rangle \tag{5}$$

where the notation $\langle x \rangle = \int_o^\infty x\, g(\tau_\sigma) d\tau_\sigma$ has been used. The magnitude of the dispersion in σ and ε' is determined by $g(\tau_\sigma)$, and the low and high frequency limits of the specific conductivity, σ_o and σ_∞, are given by

$$\sigma_o = e_o \cdot \varepsilon_s / \langle \tau_\sigma \rangle \tag{6}$$

and

$$\cdot\sigma_\infty = e_o \cdot \varepsilon_s \cdot \langle 1/\tau_\sigma \rangle \tag{7}$$

where ε_s is the high frequency limit of ε'. The low frequency limit of ε', ε_o is given by

$$\varepsilon_o = \frac{\langle \tau^2 \rangle}{\langle \tau \rangle^2} \varepsilon_s \tag{8}$$

For a single relaxation time, it is clear that $\varepsilon_o = \varepsilon_s$ and $\sigma_o = \sigma_\infty$. Electrical relaxation in ionic materials has been the subject of several recent publications. The alkali silicate glasses have been intensively studied by Macedo, Moynihan and coworkers[3-8], and also by Hakim and Uhlmann.[7] A fused anhydrous nitrate mixture has been studied by Howell et. al.[8], a hydrated calcium nitrate has been studied by Ambrus et. al.[9], and a concentrated aqueous solution has been studied by Moynihan et. al.[10] Generally, the empirical relaxation function of Williams and Watts[11a] gives a good fit to the data (see Ref. 5), although Hakim and Uhlmann[7] found that the empirical Cole-Davidson distribution function[11b] best fitted their data on Cs_2O-SiO_2 and Na_2O-SiO_2 glasses. An adequate theory for these empirical findings remains to be developed, and the determination of the complete response function for the acids was of interest in order to decide whether the protonic conductors were significantly different from these other ionic conductors.

II. Experimental Section

(a) Preparation of Solutions

All solutions were made up with distilled, deionised water ($\sigma_o \sim 10^{-6}$ δ cm^{-1} at 25°C) and reagent grade salts and acids. The salts were used

without purification, and were always taken from a freshly opened bottle. The HCl solutions were prepared by adding water to reagent grade concentrated hydrochloric acid and titrated against freshly standardised sodium hydroxide.

(b) Glass Transition Temperatures

The glass temperatures were measured by differential thermal analysis, using essentially the same technique described by Angell and Sare.[12] Calibrated chromel-alumel thermocouples were used, and were protected from corrosion by a glass sheath which was collapsed onto the junction.

(c) Electrical Conductivities

The d.c. (i.e. frequency-independent) conductivity data were obtained using a two terminal cell, described elsewhere,[13] and the frequency dependence data were obtained using an all-metal three terminal cell described elsewhere.[10] For $f \leq 500$ Hz, a modified Barberian-Cole bridge[14] was used. For 1KHz $\leq f \leq$ 20 KHz a Wayne-Kerr B221 bridge was used in conjunction with a GR 1309-A oscillator and GR 1232-A tuned amplifier and detector, and for 50KHz $\leq f \leq$ 2MHz a Wayne-Kerr 601 bridge was used in conjunction with a Wayne-Kerr SR 268 source and detectors unit. Resistance and capacitance data are accurate to < 1%, typically 0.1-0.5%.

For the initial "d.c." measurements (see later) the conductance cell was placed in a large styrofoam insulated aluminum block which was largely immersed in liquid nitrogen contained in a large dewar. Temperature control to $\sim$ 0.1°C could readily be achieved by dripping liquid nitrogen on the block from time to time. For the frequency dependence studies, the cell was placed in an ethanol-methanol bath which was cooled with a flow of cold nitrogen through a copper tube in the bath. Temperature control was generally to within ±0.2°C over the duration of a single run ($\sim$ 30 minutes). Though in

three of the runs for which data are recorded here an unchecked drift of 0.3°, 0.4° and 0.7° was tolerated. The results for these runs are of course less heavily weighted in any conclusion drawn. Plots of data for these runs are marked with an asterisk.

(d) PRM Chemical Shifts

Proton magnetic resonance spectra were recorded using a Varian A60 six turn probe spectrometer equipped with a temperature control. Temperatures were measured by insertion of a copper-constantan thermocouple into the probe. Depending on the sample composition the samples were either pre-heated by a cartridge heated aluminum block or precooled by slush baths before insertion into the probe. After insertion a period of five to ten minutes was allowed before the spectrum was recorded.

For most measurements the resonance was very sharp, since measurements were all made at temperatures sufficiently high for the solution viscosity to have no detectable effect. For one series of measurements the temperature was deliberately lowered to a region in which viscous line broadening became observable and the half-widths were determined as a function of temperature in order to derive kinetic information on the proton motion.

(e) Infrared Spectra

Infrared spectra were obtained using samples held in a standard liquid IR cell between AgBr windows, using a Perkin-Elmer model 467 extended range IR spectrophotometer. The measurements performed fell into two classes,

(i) room temperature spectra on sodium salt solutions of anions with very different basicities, performed with the objective of determining the effect of hydrogen bond strengths and the frequency and band shape of the OH stretching mode in the vicinity of 3400 cm^{-1}, and

(ii) measurements arrived at determining the effect of temperature on the IR spectra of some of the acid solutions which yield a highly conducting glass at lower temperatures, with the object of determining the types of sites, and the number of distinguishable sites, for protons on oxygen centers which exist in the solutions.

For the low temperature measurements a variable temperature enclosure for the liquid cell was constructed, using gas cooling of the cell within a styrofoam housing, as the temperature-regulating principle. Nitrogen was used as the heat transfer gas. It was circulated through a coil immersed in a liquid nitrogen dewar to establish a lower temperature base and then pre-heated prior to entry to the cell to the desired temperature by means of a Cole-Palmer thermistor controlled regulator. This arrangement sufficed to maintain the temperature in the cell constant to ± 1°C during the course of a spectral recording.

Results

Many of the results presented in this section have been given previously in a technical report on this project. The areas in which new results have been obtained are

(i) frequency dependence of the electrical conductance,

(ii) pure chemical shifts and

(iii) the spectral investigation of the hydrogen bond stretching mode line-width.

(a) D.C. Conductivities

Results for the d.c. conductance at T_g in the $Li_2Cr_2O_7 \cdot 6H_2O$ + $H_2Cr_2O_7 \cdot 6H_2O$ system are shown in Fig. 1. It is noted that there is a dramatic decrease, amounting to some three orders of magnitude in the conductance as

35% of the protons are replaced by lithium ions. A simple dilution effect would be expected to produce only linear decreases. Thus, it would appear not only that the protons are dominating the conduction mechanism in the acid glass but that the presence of water-reorienting impurities such as lithium ion are very destructive to the mechanism. An interpretation is that the lithium orientates the water molecules around it in a way which renders them unsuitable for the Gyrotthus type chain conduction mechanism by which the protons must move if they are to exhibit an anomalous mobility.

More will be said of this below. The essential result at this point is that the presence of protons in excess quantities are clearly needed if a large conductance at the glass temperature is to be manifested.

To answer the question of what types of acids can provide a high proton conductivity, we present data for a number of different acids, all studied at their respective glass temperatures, in Table 1. The Table 1 results would imply that simply the use of a strong acid is insufficient to lend high protonic conductivity at the glass temperature. The case of $HCl \cdot 6H_2O$ suffices to make this point since HCl is unquestionably a strong acid, yet its conductance at T_g is essentially that of the $LiCl \cdot 6H_2O$ solution which is considered to approximately represent the condition of zero excess of conductivity over that expected from ionic contributions.

(b) Frequency Dependent Conductance Studies

In order to determine with more detail the conductance mechanism, and to make comparisons with other ionic conducting glasses, the conductance of selected proton-conducting glasses was studied as a function of frequency at various temperatures both above and below the value of T_g determined by dta experiments. Capacitance measurements were recorded simultaneously and

the results combined with the conductance measurements to deduce the real and imaginary parts of the electrical modulus, M^*, defined in the introductory section.

Results for the conductance, and the derived electrical moduli components are shown in Figs. 3-21, for the following acid solutions:

(i) $H_2ZnCl_4 \cdot 10\ H_2O$

(ii) $H_2ZnCl_4 \cdot 12\ H_2O$

(iii) $H_3Zn_2Cl_7 \cdot 12\ H_2O$

(iv) $HZnCl_3 \cdot 4H_2O$

(v) $HZn_2Cl_5 \cdot 4H_2O$.

The lines drawn through the points are plots of real and imaginary parts of the dielectric moduli based on Cole-Davidson distribution functions the parameters for which are presented in Table 2 of this report.

(c) PMR Chemical Shifts

PMR chemical shifts and their temperature dependence have been measured for a large number of protonic acids, including those for which the above conductance studies have been made. The results are presented in a graph, Fig. 22 in which the magnitude of the shift relative to tetramethyl ammonium ion, and its temperature dependence, is plotted against the pKa for the acid. This plotting parameter refers to the properties of the acid at infinite dilution, and represents the ability of the anion to withhold a proton from water molecules in the bulk solvent i.e. its hydrogen bonding ability. Fig. 9 suggests that the deshielding of the protons in the concentrated acid solutions under study remains dominated by the hydrogen bonding ability of the anionic component of the solution, in the case of weak acids although the correlation is very poor. In the case of the strong acids which yield conducting glasses

according to the above recorded conductivity studies, Fig. 9 suggests the protons are essentially completely transferred to the water molecules present in the liquid. The temperature dependence of the shift is clearly greater for those acids in which the hydrogen bond to the anion is strong than it is for the solutions which form conducting glasses. The correlation with pKa is very poor for the acids of known pKa is very poor.

Proton Magnetic Resonance Line-Width Studies

PMR measurements will give distinct resonances for protons in different magnetic environments if the exchange time for protons between such sites is with respect to the reciprocal RF frequency (60 megahertz on the instrument at Purdue). For a single resonance line, the dependence of linewidth on temperature is determined in the temperature range of our measurements by the spin-lattice relaxation time, the value of which is usually quite closely related to the solution viscosity.

We have conducted measurements on several solutions in the range 300-180K. We find only one resonance line in each case, indicating that water protons and "free" protons exchange on time scale short with respect to 10^{-7} seconds even at the lowest temperatures.

The linewidth however is very temperature-dependent. For two solutions the half-width is plotted as 1/T in Fig. 23. At all temperatures the half-width is smaller, hence the relaxation time shorter, for the solution containing "free" protons. The shape of the relaxation time reciprocal temperature plot is characteristic for relaxation times in viscous liquids. The linewidth becomes too broad to measure at a temperature well above T_g.

(d) Infrared Spectral Studies

Because the IR time scale is of the order of inverse vibration frequencies no motional averaging of discrete site absorptions occurs and if different

proton-oxygen sites exist they will be detected through their different O-H stretching and rocking frequencies.

We have now conducted trial experiments in which the IR spectra from 200-4000 cm^{-1} have been obtained at temperatures over the range 30 to -150°C for the most important of the proton-conducting solutions. These are shown in condensed form in Fig. 11 for the system $HZnCl_3 \cdot 4H_2O$, which has good glass-forming properties. The procedure was to cool the glass film (in an AgBr cell) to -150°C initially, and then to record spectra at various constant temperatures during reheating to room temperature.

The sharpened spectra seen at -77°C and -45°C are presumably due to partial crystallization which occurred in this range. Which crystal forms are obtained are yet to be determined, but they will no doubt be useful in determining whether H_3O^+ or $H_6O_2^+$ species are dominant in these liquids. Spectra for $H_2SO_4 \cdot H_2O$ and $3H_2SO_4 \cdot H_2O$ solutions suggest H_3O^+ is the preferred proton-carrying entity, but the spectra have not to date been analyzed in sufficient detail for this to be certain.

The spectra all seem to show the development of a bands at ∿1700 cm^{-1} and 11-1200 cm^{-1} as the principal departures from the spectra of ordinary water. The band at ∿3500 cm^{-1} is shifted in frequency. This is the only band which is significantly shifted by temperature in the system shown. HNO_3 solutions show a greater temperature dependence, but their proton conducting ability in the glassy state has not yet been studied.

OH Stretching Mode Band Width Studies

IR spectra in the frequency range 400-4000 cm^{-1} have been recorded for the following solutions (at room temperature unless otherwise indicated):

(a) (i) Na_2CO_3 (20R), (ii) Na_2HPO_4 (20R), (iii) Na_2HPO_3 (20R),

(iv) Na_2CrO_4 (20R), (v) Na_2SiO_3 (20R), (vi) $Na_2S_2O_3$ (20R), (vii) $NaCH_3COO$ (10R), (viii) $NaHSO_3$ (10R), (ix) $NaCCO_3$, (x) $NaNO_3$ (10R), (xi) NaCl (10R), (xii) NaN_3 (10R), (xiii) $NaCCO_4$ (10R).

(b) (i) HF (64R), (ii) HF (8R) T = 25°, -45°, -157°; (iii) HNO_3 R = 10, T = 25°, -130°; (iv) $HZnCl_3$ (4R) T = 17°, -13°, -45°, -77°, -98°, -116°, -145°; (v) H_2ZnCl_4 (10R) T = 25°, T = -121°.

The solutions listed under (a) above were chosen for the common cation but different anions they contain so that the effectiveness of the anion in "loosening" the proton on adjacent water molecules could be studied. A selection of these is shown in Fig. 24. It is to be noted that the band width is much broader in the case of anions of high proton attracting abilities (large basicities) than in solutions with anions of low proton attracting abilities. The trend, however, is not very well defined, and attempts to correlate the band width with the pKa parameter have not proved successful.

Discussion Section

D. C. Conductivities

Fig. 1 indicates that the conductivity mechanism for all of the acids is the same, and that the "structures" of the systems at their particular T_g's are very similar. (The word "structure" is here meant to reflect the time scale of the structural relaxation of the system, as well as the average arrangement of the particles in it.) The reason the acid $HZn_2Cl_5 \cdot 4H_2O$ does not lie on the straight line the others do is, possibly, that the oligiomeric or polymeric anions disrupt the proton transfer mechanism. Such a disruption would also account for

the large rms jump length derived via the Nerust-Einstein equation for this acid (1.3Å compared to $\sim$ 0.8Å for the other acids, see below).

The calculated values of the rms jump distance are all reasonable. In water, proton transfers between suitably oriented water molecules involve a jump distance of $\sim$ 0.3Å,[15] and it is usual to average this with an intramolecular transfer distance of $\sim$ 3Å.[16] Because the dielectric relaxation of water, 10^{-11} sec,[17] is so much larger than the lifetime of H_3O^+, $\sim 10^{-13}$ sec,[15,18] it can be assumed that the proton sees a frozen structure when it jumps and that the above estimates of jump distances may be reasonably compared with the estimates reported here. The average jump distance of $\sim$ 0.8Å is a reasonable average of 0.3Å and 3Å.

The Fictive Temperature

It should be noted that the T_g's referred to in this discussion are those determined by d.t.a. i.e. they are determined at the same heating rate ($\sim$ 10°C min^{-1}) on materials which were quenched at the same rate ($\sim$ 20°C sec^{-1}). The structural relaxation time at these T_g's are thus the same for all the acids. The effective T_g of the acids during a conductance experiment, however, is lower than the d.t.a. T_g because the conductance cell was equilibrated for at least an hour or so before measurements were made. The "annealed" T_g of the acids therefore corresponds to a structural relaxation time of 30 minutes or so.

Howell et. al.[8] have recently reported the d.c. conductivities of a glass-forming fused salt mixture (40 mol % $Ca(NO_3)_2$-60 mol % KNO_3) above and below a precisely established annealed T_g, and observed a distinct change in activation energy at this T_g (from 78 kcal $mole^{-1}$ in the liquid to 24 kcal $mole^{-1}$ in the glass). They interpreted this in

terms of the fictive temperature, T_f, which they say "may be thought of as the temperature at which the structure of the system would be an equilibrium structure." We give a brief summary of their important results and apply them to the data reported here.

The conductivity is expressed functionally as

$$\sigma_o = \sigma_o(T, T_f) \tag{13}$$

and the activation enthalpy, ΔH^*, is given by

$$\Delta H^* = - R \frac{d\ln\sigma_o}{d(1/T)} \tag{14a}$$

$$= - R\left[\frac{\gamma\ln\sigma_o}{\gamma(1/T)}\right]_{T_f} - R\left[\frac{T^2}{T_f^2}\right]\left[\frac{\gamma\ln\sigma_o}{\gamma(1/T_f)}\right]_1\left(\frac{dT_f}{dT}\right) \tag{14b}$$

$$= \Delta H_1 + \Delta H_2 \tag{14c}$$

For the liquid above T_g, $T_f = T$, $dT_f/dT = 1$ and both ΔH_1 and ΔH_2 contribute to ΔH^*, provided $[\gamma\ln\sigma_o/\gamma(1/T_f)]$ is not zero. For the glass below T_g the structure is frozen on the experimental time scale, T_f is constant, $dT_f/dT = 0$ and only ΔH_1 contributes to ΔH^*.

The activation energy of 8.5 kcal mole^{-1} (Fig. 1) clearly corresponds to ΔH_1. If the "structure" (as defined above) is measured by the configurational entropy S_c for example (and for substances as similar to one another as these acids, this is not unreasonable), then insofar as T_g determines S_c and the latter is the same at the d.t.a. T_g for all the acids, T_f is constant. Consider, as a working equation for illustrative purposes only, the Adam-Gibbs[19] expression

$$\sigma_o = A \exp\left[-B/RTS_c(T_f)\right] \tag{15}$$

where A and B are constants. If it is assumed that $S_c(T_f)$ is given by

$$S_c(T_f) = \Delta C_p \ln(T_f/T_o), \tag{16}$$

where ΔC_p is the temperature independent configurational heat capacity and T_o the temperature at which S_c vanishes at equilibrium, and if it is also assumed that A, B and ΔC_p are the same for all the acids, then $T_g(dta)/T_o$ is the same for all the acids, $dT_f/dT_g = 0$, and Fig. 1 does, in fact, measure ΔH_1. However, since S_c is changing with temperature at $T_g(dta)$, the temperature dependence of σ_o for a particular acid at its T_g is characterised by an activation energy of $\Delta H_1 + \Delta H_2$. The activation energies measured at the dta T_g for the acids of this study are comparable because the acids are so similar in "structure", and ΔH_2 as well as ΔH_1 is essentially the same for them all.

Because problems of sample cracking were anticipated far below $T_g(dta)$, most of the relaxation data were not taken sufficiently below $T_g(dta)$ to test the prediction that the activation energy should approach ~ 8.5 kcal mole^{-1} in the frozen glassy state. The data for $HZnCl_3$ (see Fig. 26), however, extend to low enough temperatures to indicate that the activation energy is beginning to approach a value close to 8.5 kcal mole^{-1}. Actually, because ΔH_1 varies inversely with $S_c(T_f)$*, it is expected that ΔH_1 (annealed T_g) > ΔH_1(dta T_g), and Fig. 12 shows that the low temperature activation energy appears to be somewhat higher than 8.5 kcal mole^{-1}. It is interesting and significant to note that the conductivity activation energy in ice is 12.7 kcal mole^{-1},[20] comparable to ΔH_1 for the acids. Parenthetically, the high activation energy for surface conduction in ice of 37 kcal mole^{-1}[20] appears to be a good example of the ideas discussed above, since the slow freezing of a surface layer of water has been suggested as being responsible for the large activation energy for conductivity of ice.[20]

*The Adam-Gibbs theory predicts that $\Delta H_1 = B/S_c(T_f)$.

Electrical Relaxation Behavior

Figs. 11, 14 and 17 show that there is an absorption in excess of that predicted by the Cole-Davidson function, at high frequencies. This is possibly due to a β relaxation, which appears at high frequencies for a wide variety of glasses,[21] but it does not appear to be sufficiently well defined to warrant further attention. A low frequency dispersion in conductivity was observed for some of the acids at and below T_g(dta). This is probably due to an air gap at the electrode surface, but does not affect the data other than to increment M' by a constant amount and, possibly, give a weak shoulder on the low frequency side of the M' peak. Overall, however, the Cole-Davidson function gives a very good fit to the data (see Ref. 22 for plots of all the data).

Although the Cole-Davidson function has not been much used in fitting conductivity relaxation in glasses, it does give a good overall fit of data for a wide variety of systems. To illustrate this, we show in Fig. 27 a comparison of the Cole-Davidson fits with William-Watts[11] and double log gaussian[4] fits of literature data. It is seen that in some cases the Cole-Davidson function gives a better fit than the functions the various authors chose to use. Because amorphous ionic conductors can be generally characterized by the Cole-Davidson function, and because diffusion plays such a fundamental role in conductivity relaxation, we discuss the data in terms of the Glarum defect diffusion model,[23] which predicts a relaxation function which is very similar to the Cole-Davidson function.

The model assumes a cooperative relaxation process, which is treated in terms of defects diffusing to a relaxing dipole. The dipoles relax

with a single relaxation time T_R, but relax completely and instantly upon arrival of a defect. The model incorporates a shape factor a_o, which is related (to a good approximation) to the Cole-Davidson γ parameter by

$$\gamma = a_o^{1/2}/(1 + a_o^{1/2}) \qquad (17)$$

The parameter a_o is the ratio of the diffusional relaxation time to T_R. For most amorphous materials in the supercooled liquid or glassy states, $0.2 < \gamma < 0.5$ so that $0.125 < a_o < 1.0$.

In applying the model to conductivity relaxation, it is necessary to specify the nature of both the relaxing dipole and the diffusing defect. One possibility is to treat the defects as the diffusing ions themselves and the relaxing dipole as a buildup of charge either side of a potential energy barrier (see, e.g., ref. 3). The "dipole" may relax in two ways, either by an ion jumping over the barrier (single relaxation time), or by another ion diffusing to the barrier, via jumps over other lower energy barriers. The two relaxation times would be expected to be comparable ($a_o \sim 1$), but because of their traversal over lower barriers the diffusing ions have a shorter relaxation time (i.e. $a_o < 1$, in accord with experiment). At lower temperatures, only the ions crossing lower barriers contribute to the relaxation, so that a_o should increase with decreasing temperature (i.e. the loss peaks narrow with decreasing temperature, as observed).

The idea of identifying the Glarum defects, with ions, although crude, would seem to be worthy of more serious study.

Conclusion

It is clear that electrical relaxation in these protonic conductors is determined by the same fundamental mechanism which determines the relaxation in other amorphous ionic conductors, viz. a random hopping of

charged particles. It seems immaterial whether the ions reside on specific chemical entities (such as protons on water molecules) or if they reside in the interstices of a connected lattice structure (such as alkali ions in a silicate network). Any type of band theory for these protonic conductors is ruled out.

The mobile protons are presumed to be those resident on oxygens bearing three protons (H_3O^+), for which, according to IR spectra, there is a single quite well defined potential surface. Exchange between these protons and those on doubly occupied oxygens is, however, rapid on the NMR time scale. Whether or not a particular acid glass is a good conductor at T_g, would appear to depend more on the absolute value of T_g, hence on the state of vibrational or librational excitation of the excess proton-bearing species, than on the strength of the acid (provided the site on H_3O^+ is at a lower energy than that on the anion).

REFERENCES

1. C. A. Angell, R. D. Bressel, and P. M. Gammell, J. Non. Cryst. Solids, 7, 295 (1972).
2. A. J. Easteal and C. A. Angell, J. Electrochem. Soc., 120, 1143 (1973).
3. P. B. Macedo, C. T. Moynihan and R. Bose, Phys. Chem. Glasses, 13, 171 (1972).
4. V. Provenzano, L. P. Boesch, V. Volterra, C. T. Moynihan, and P. B. Macedo, J. Amer. Ceram. Soc., (in press).
5. C. T. Moynihan, L. P. Boesch and N. L. Laberge, Phys. Chem. Glasses, (in press).
6. L. P. Boesch and C. T. Moynihan, J. Non. Cryst. Solids, submitted.
7. R. M. Hakim and D. R. Uhlmann, Phys. Chem. Glasses, 14, 81 (1973).
8. F. S. Howell, R. A. Bose, P. B. Macedo and C. T. Moynihan, J. Phys. Chem., 78, 639 (1974).
9. J. H. Ambrus, C. T. Moynihan and P. B. Macedo, J. Phys. Chem., 76, 3287 (1972).
10. C. T. Moynihan, R. D. Bressel and C. A. Angell, J. Chem. Phys., 55, 4414 (1971).

11a. G. Williams and D. C. Watts, Trans. Faraday Soc., 66, 80 (1970).

11b. R. H. Cole and D. W. Davidson, J. Chem. Phys., 18, 1417 (1951).

12. C. A. Angell and E. J. Sare, J. Chem. Phys., 52, 1058 (1970).
13. R. D. Bressel, Ph.D. Thesis, Purdue University (1972).
14. J. G. Barberian and R. H. Cole, Rev. Sci. Instr., 40, 811 (1969).
15. B. E. Conway et. al., J. Chem. Phys., 24, 834 (1956).
16. L. J. Gagliardi, J. Chem. Phys., 58, 2193 (1973).
17. C. H. Collie et. al., J. Chem. Phys., 16, 1 (1948).

18. E. Wicke et. al., Z. Phys. Chem. (Neve Folge), 1, 340 (1954).

19. G. Adam and J. H. Gibbs, J. Chem. Phys., 43, 139 (1965).

20. M. A. Maidique, A. von Hippel and W. B. Westphal, J. Chem. Phys., 54, 150 (1970).

21. G. P. Johari and M. Goldstein, J. Chem. Phys., 53, 2372 (1970).

22. I. M. Hodge, Ph.D. Thesis, Purdue University (1974).

23. S. H. Glarum, J. Chem. Phys., 33, 639 (1960).

TABLE 1

D. C. CONDUCTIVITIES

Substance	Composition $n(H_2O)$	T_g(K)	σ_o
LiCl	6	137.7	2.0×10^{-12}
$H_2Cr_2O_7$	6	161.9	4.0×10^{-9}
HCl	6	127.7	2.0×10^{-12}
H_2SO_4	2	163.4	1.2×10^{-11}
H_2SO_4	1	175.5	8.0×10^{-11}
H_2SO_4	0.33	167.2	1.4×10^{-11}
H_2ZnCl_4	10	151.5	3.1×10^{-10}
H_2ZnCl_4	12	147.2	2.0×10^{-10}
$H_3Zn_2Cl_7$	12	163.9	4.0×10^{-9}
HPF_6	?	?	?
$HClO_4$	?	?	?

Table 2

Cole-Davidson Parameters

Solution	Temperature	γ	M_s
$HZn_2Cl_5 \cdot 4H_2O$	- 75.0	0.230	0.1023
	- 81.7	0.200	0.1249
	- 85.0	0.300	0.1012
	- 87.8	0.298	0.1071
	- 95.3	0.354	0.1100
	-101.0	0.384	0.1102
	-106.8	0.366	0.1040
$HZnCl_3 \cdot 4H_2O$	- 96.3	0.234	0.1072
	- 99.7	0.254	0.1072
	-103.0	0.260	0.1120
	-105.0	0.324	0.1062
	-109.0	0.364	0.1017
	-118.7	0.382	0.1023
$H_3Zn_2Cl_7 \cdot 12H_2O$	-108.3	0.250	0.1261
	-113.8	0.330	0.1137
	-115.0	0.344	0.1120
$H_2ZnCl_4 \cdot 10H_2O$	-121.3	0.200	0.1640
	-127.0	0.240	0.1380
$H_2ZnCl_4 \cdot 12H_2O$	-127.0	0.270	0.1650
	-130.3	0.240	0.1520
	-132.3	0.240	0.1520

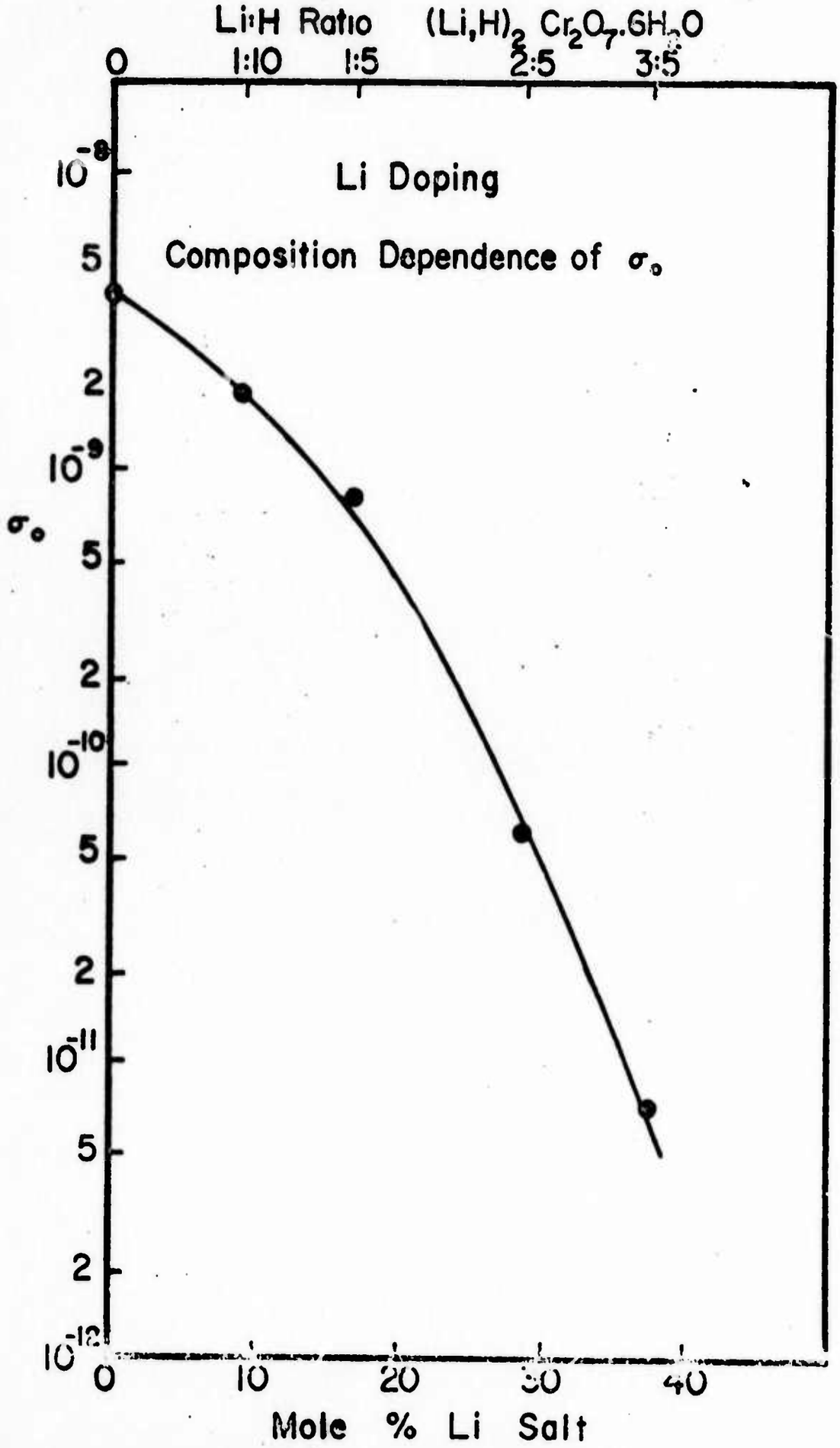
Li:H Ratio (Li,H)2 Cr2O7.6H2O
0
1:10
1:5
2:5
3:5
Li Doping
Composition Dependence of σo
σo
10-8
5
2
10-9
5
2
10-10
5
2
10-11
5
2
10-12
0
10
20
30
40
Mole % Li Salt

Fig 1

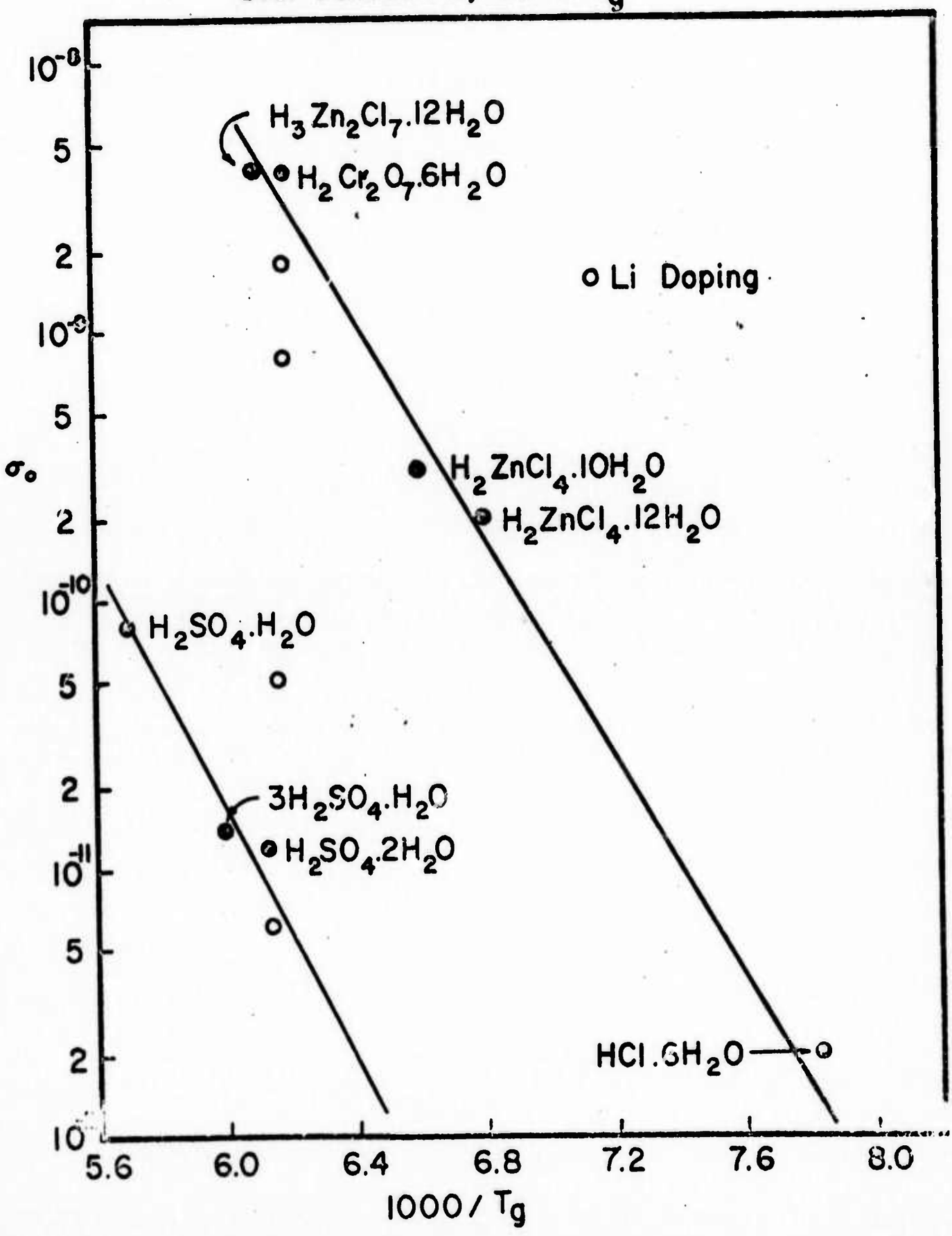
D.C. Conductivity vs. $1/T_g$
10^{-8}
5
2
10^{-9}
5
σ_o
2
10^{-10}
5
2
10^{-11}
5
2
10^{-12}
$H_3Zn_2Cl_7.12H_2O$
$H_2Cr_2O_7.6H_2O$
o Li Doping
$H_2ZnCl_4.10H_2O$
$H_2ZnCl_4.12H_2O$
$H_2SO_4.H_2O$
$3H_2SO_4.H_2O$
$H_2SO_4.2H_2O$
$HCl.6H_2O$
5.6
6.0
6.4
6.8
7.2
7.6
8.0
$1000/T_g$

Fig. 2.

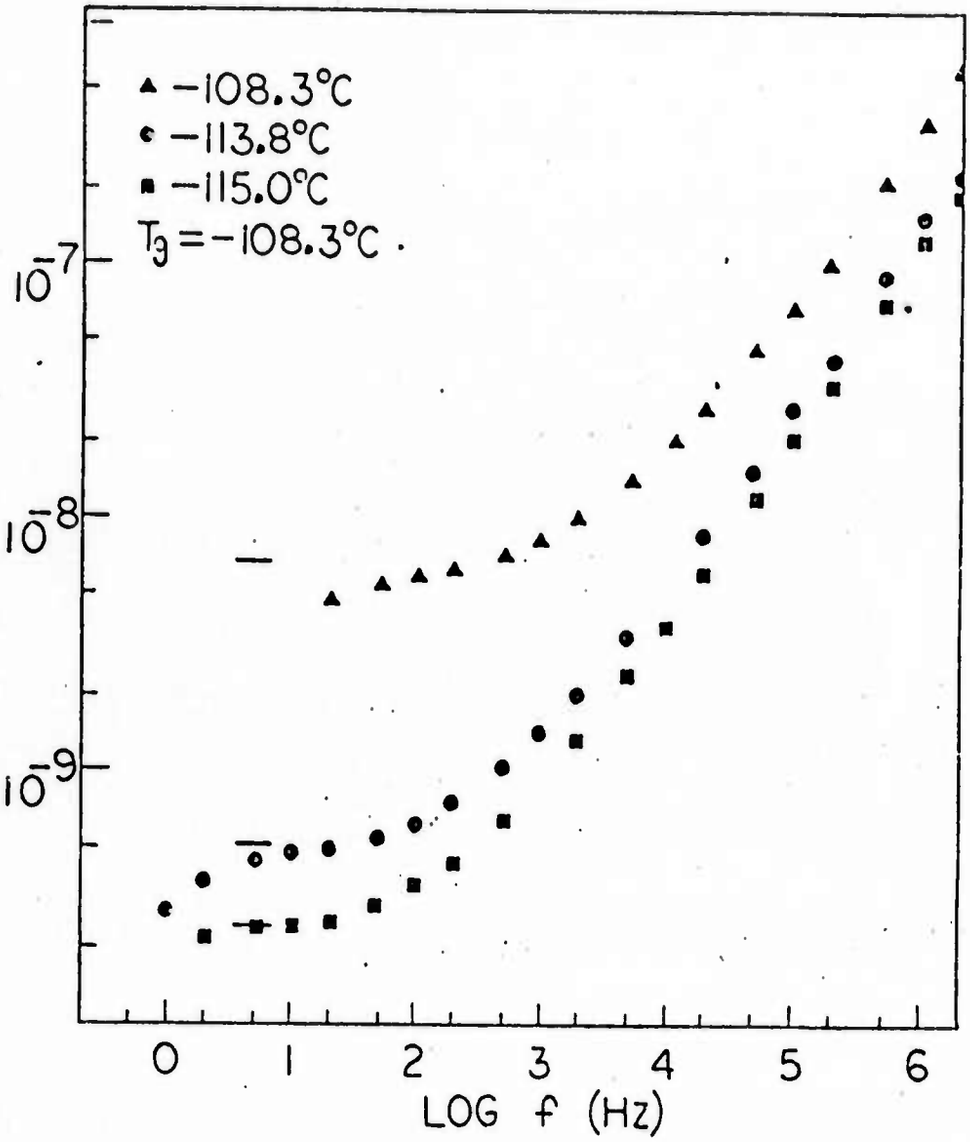

Figure 3

Specific Conductivity Frequency Dependences

for $H_3Zn_2Cl_7.12H_2O$

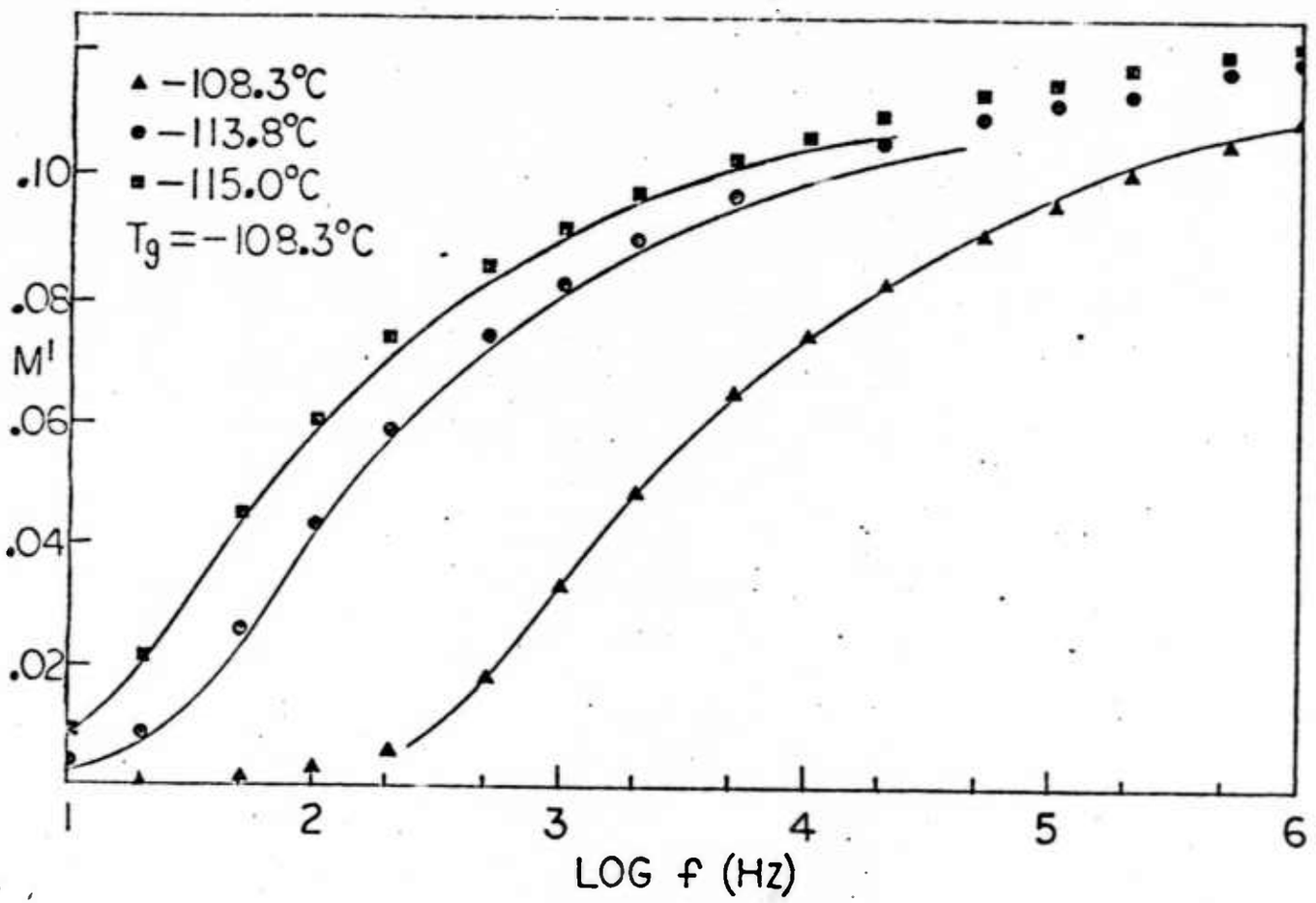

Figure 4

Cole-Davidson fits to the Frequency Dependences of Real Component of Dielectric Modulus for $H_3Zn_2Cl_7.12H_2O$

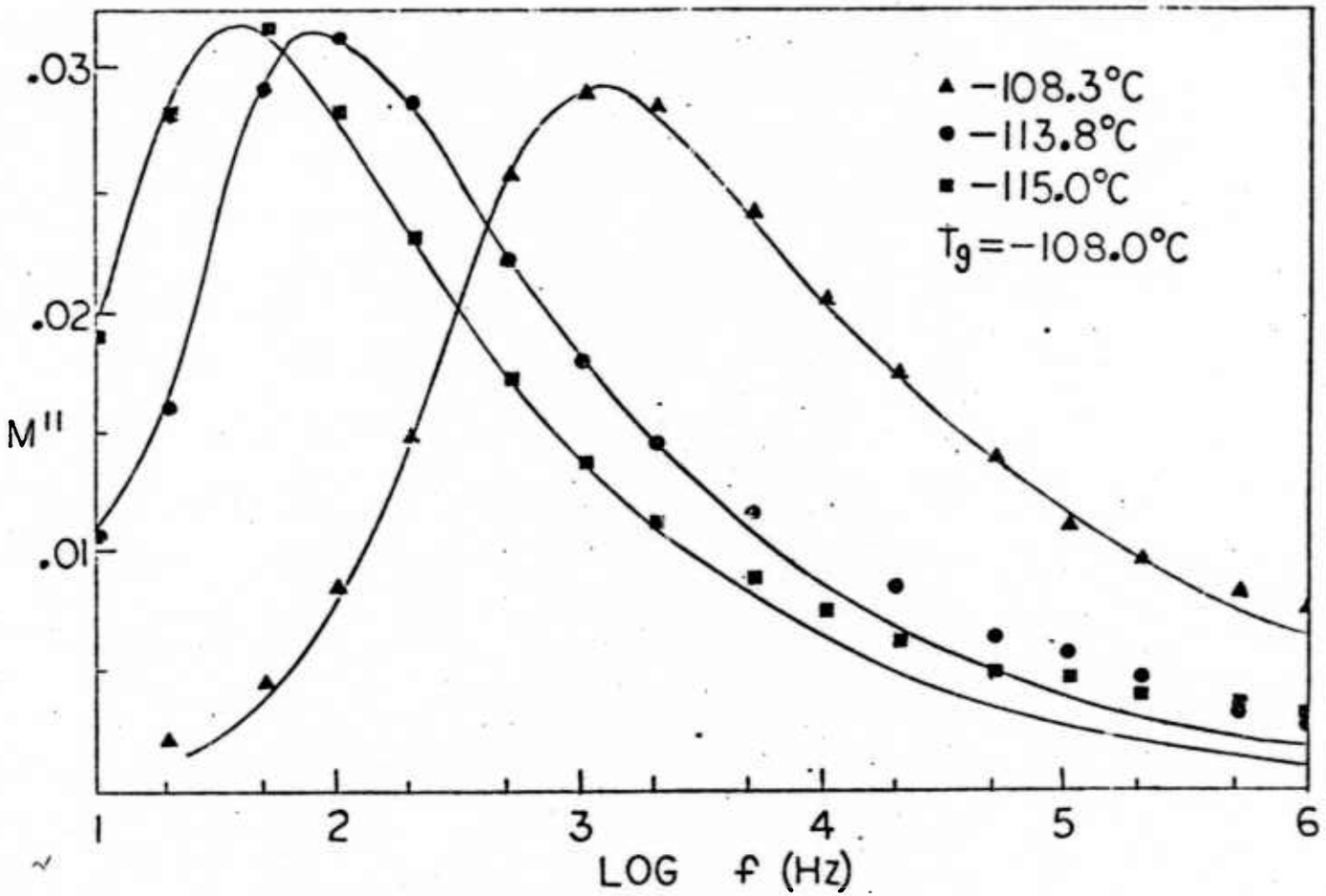

Figure 5

Cole-Davidson fits to the Dependences of Imaginary Component of Dielectric Modulus for $H_3Zn_2Cl_7.12H_2O$

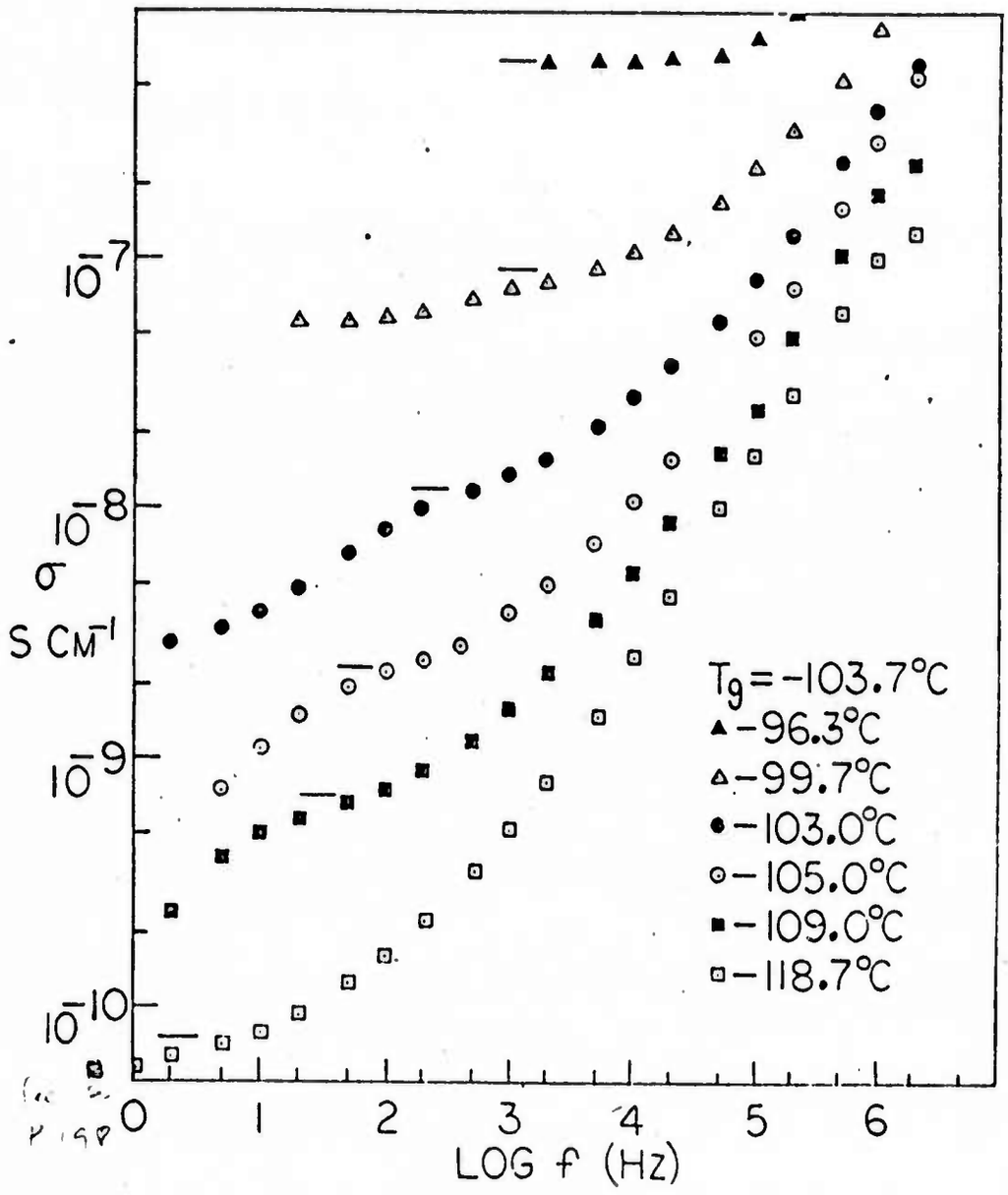

Figure 6

Specific Conductivity Frequency Dependences

for $HZnCl_3.4H_2O$

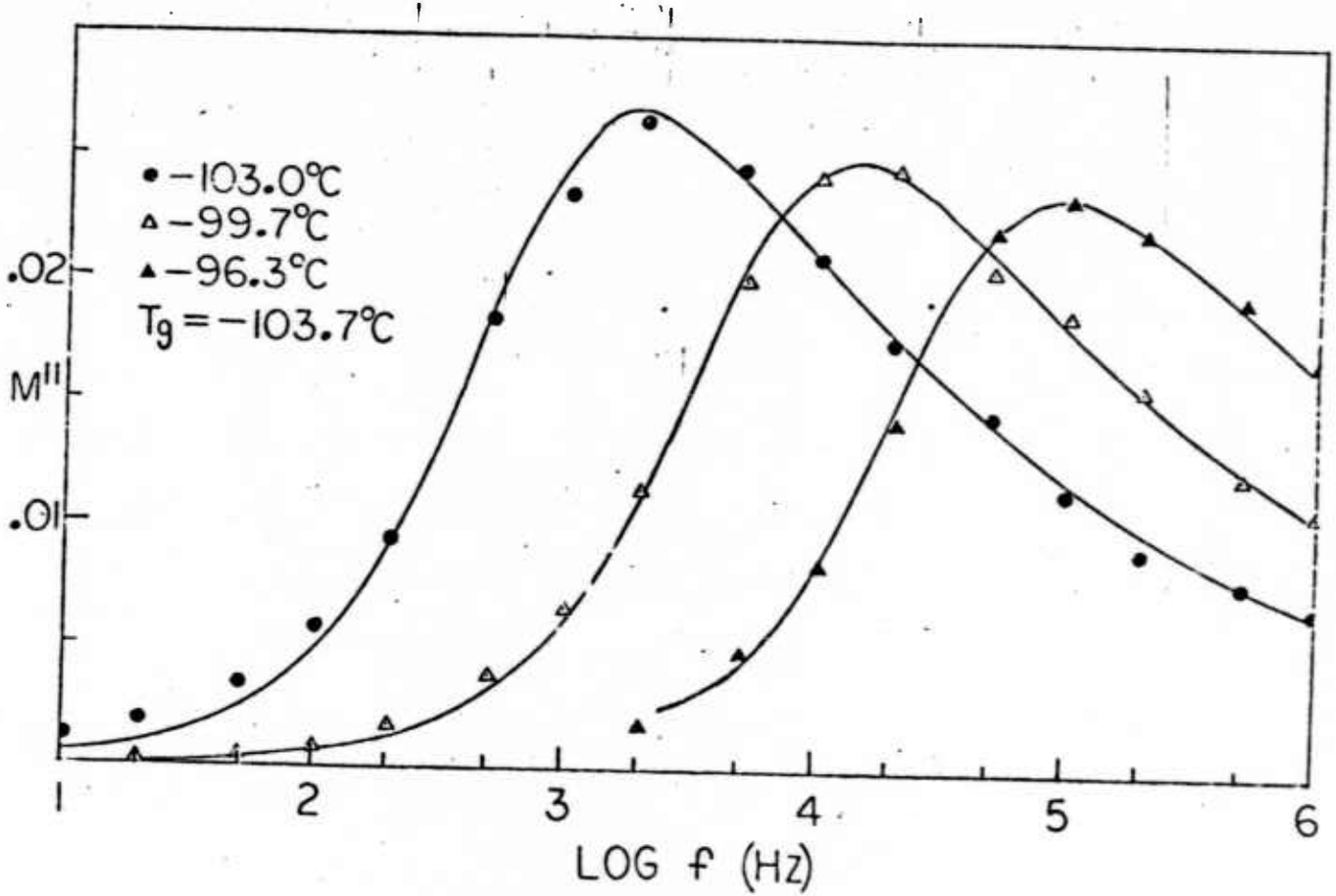

Figure 7

Cole-Davidson fits to the Frequency Dependences of Imaginary Component of Dielectric Modulus for $HZnCl_3.4H_2O$

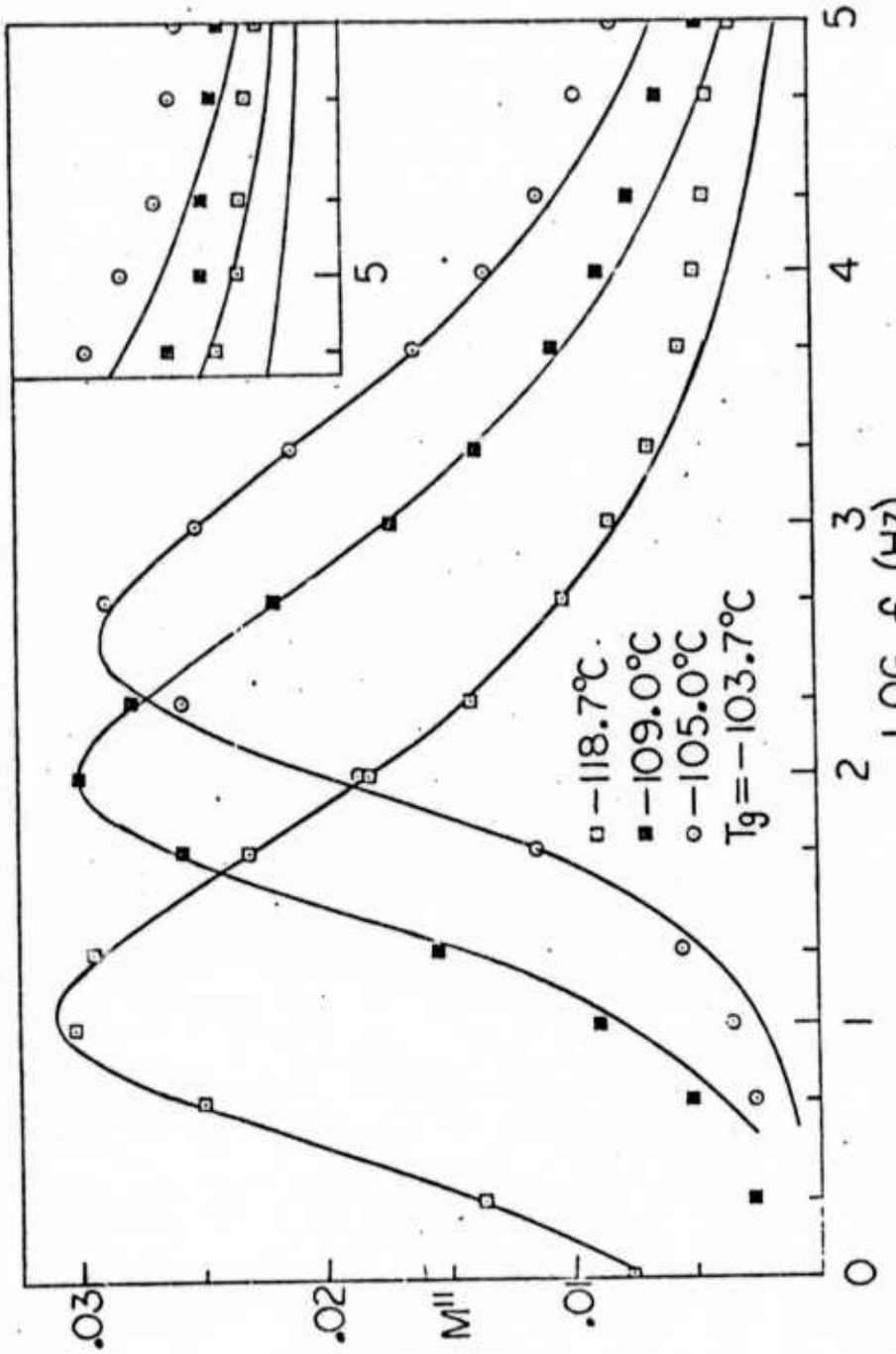

Figure 8

Cole-Davidson fits to the Frequency Dependences of Imaginary Component of Dielectric Modulus for $HZnCl_3 \cdot 4H_2O$

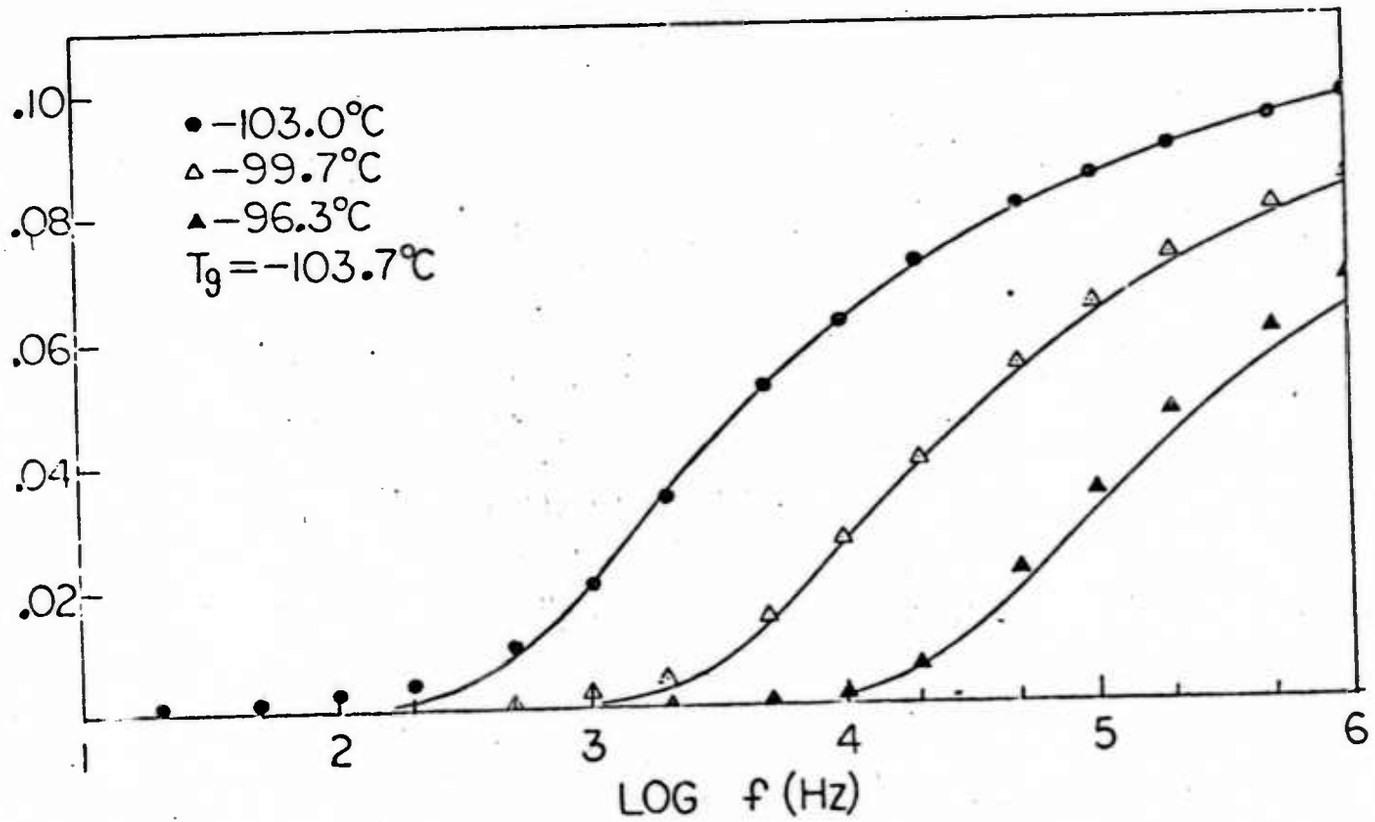

Figure 9

Cole-Davidson fits to the Frequency Dependences of Real Component of Dielectric Modulus for $HZnCl_3.4H_2O$

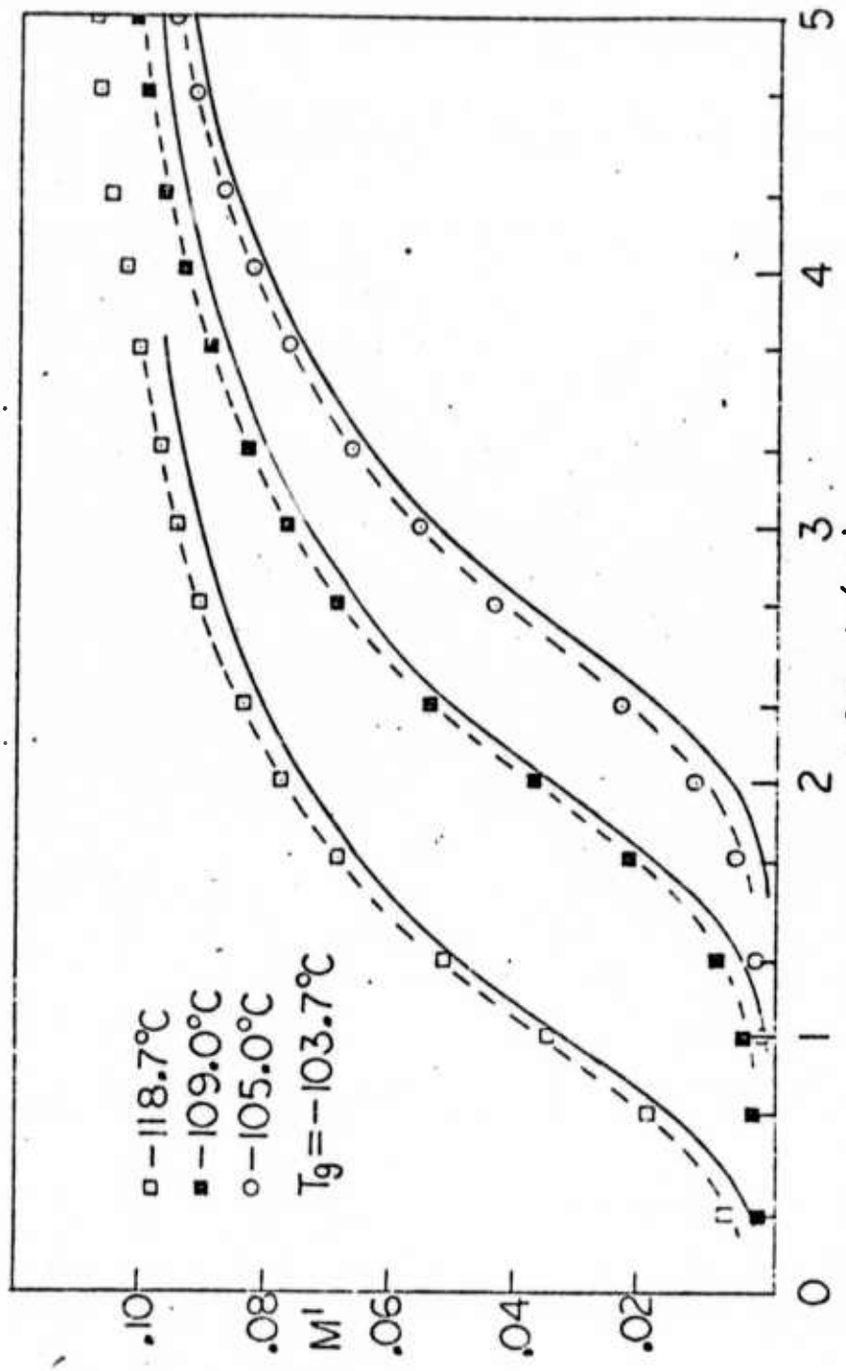

Figure 10

Cole-Davidson fits to the Frequency Dependences of Real Component of Dielectric Modulus for $HZnCl_3 \cdot 4H_2O$

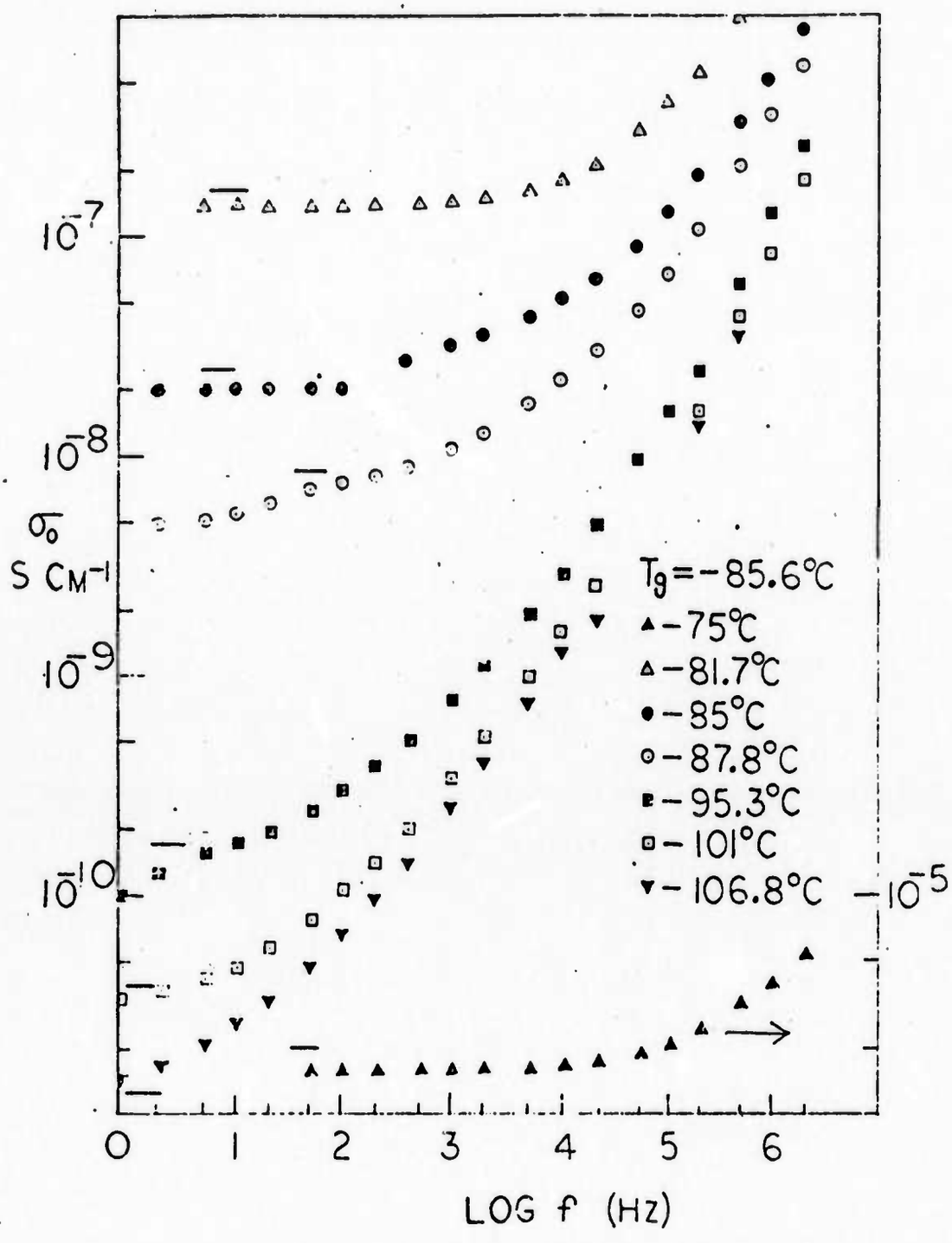

Figure 11

Specific Conductivity Frequency Dependences for $HZn_2Cl_5.4H_2O$

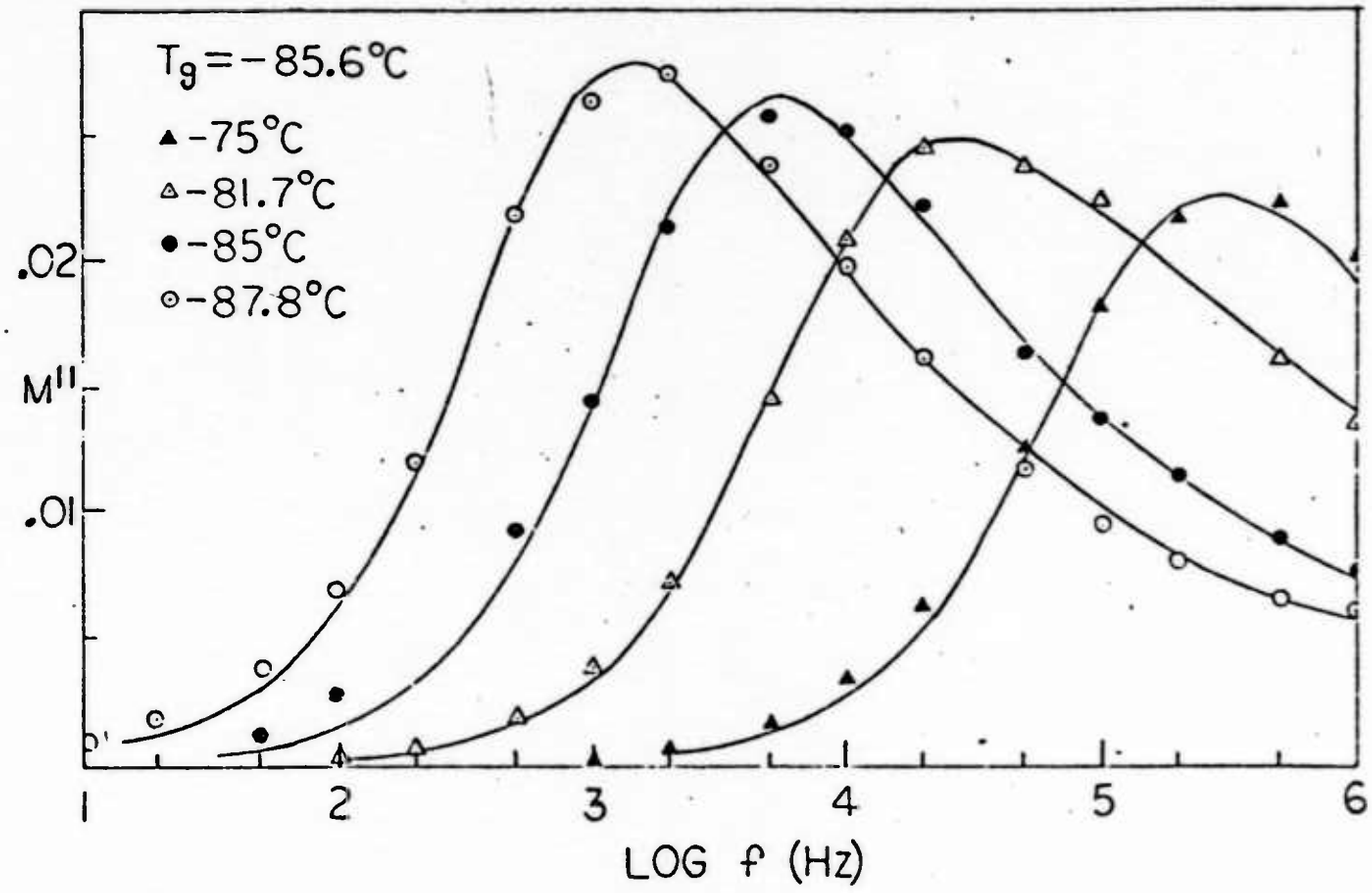

Figure 12

Cole-Davidson fits to the Frequency Dependences of Imaginary Component of Dielectric Modulus for $HZn_2Cl_5.4H_2O$

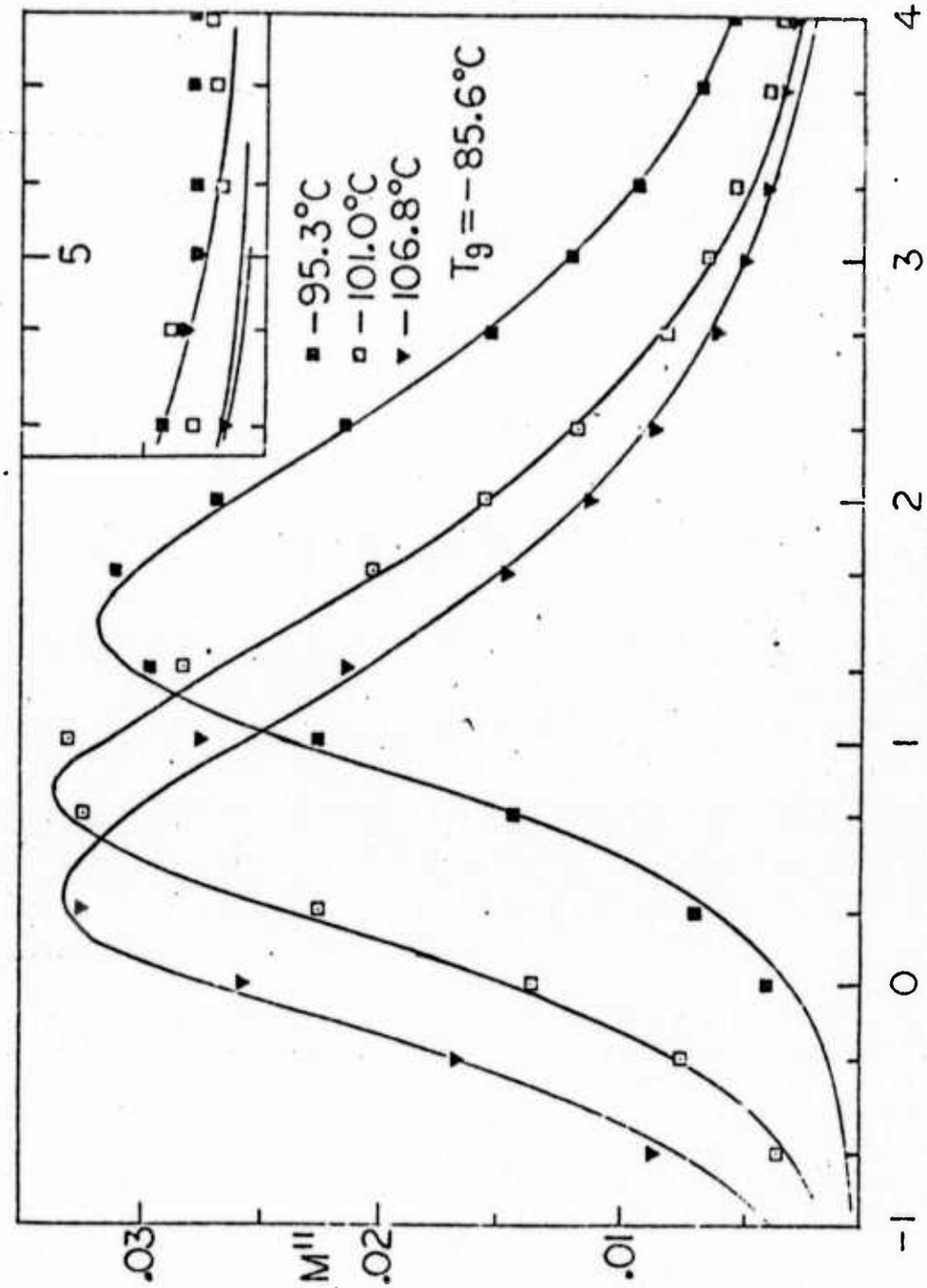

Figure 13

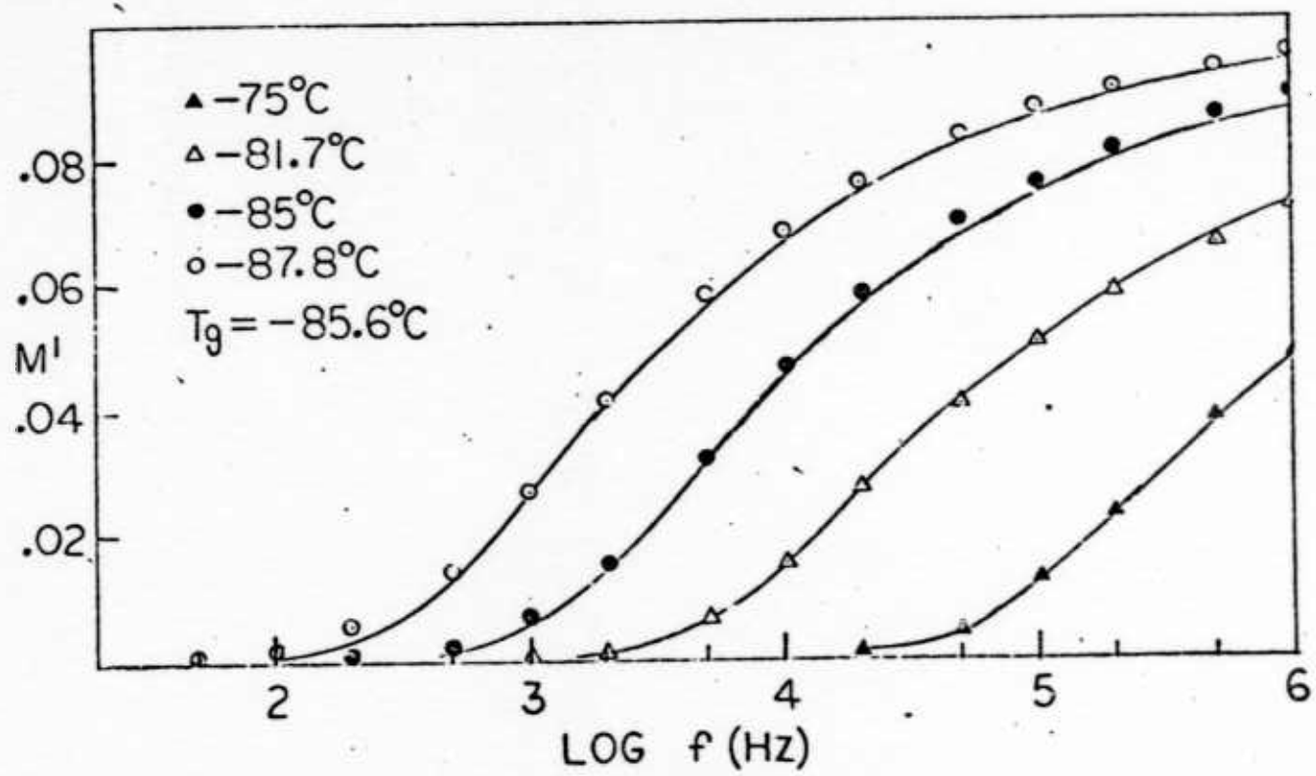

Figure 14

Cole-Davidson Fits to the Frequency Dependences of Real Component of Dielectric Modulus for $HZn_2Cl_5.4H_2O$

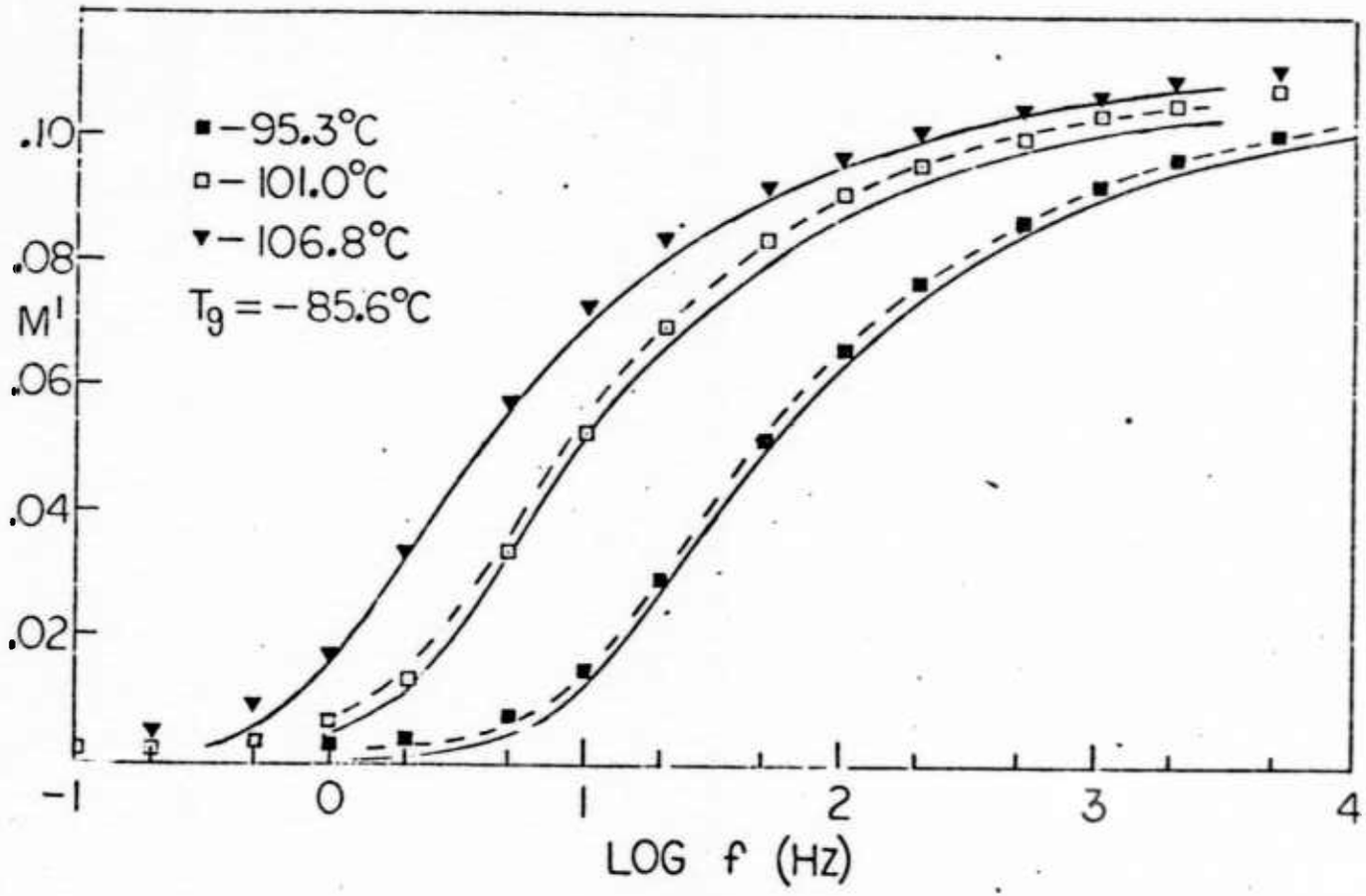

Figure 15

Cole-Davidson Fits to the Frequency Dependences of Real Component of Dielectric Modulus for $HZn_2Cl_5.4H_2O$

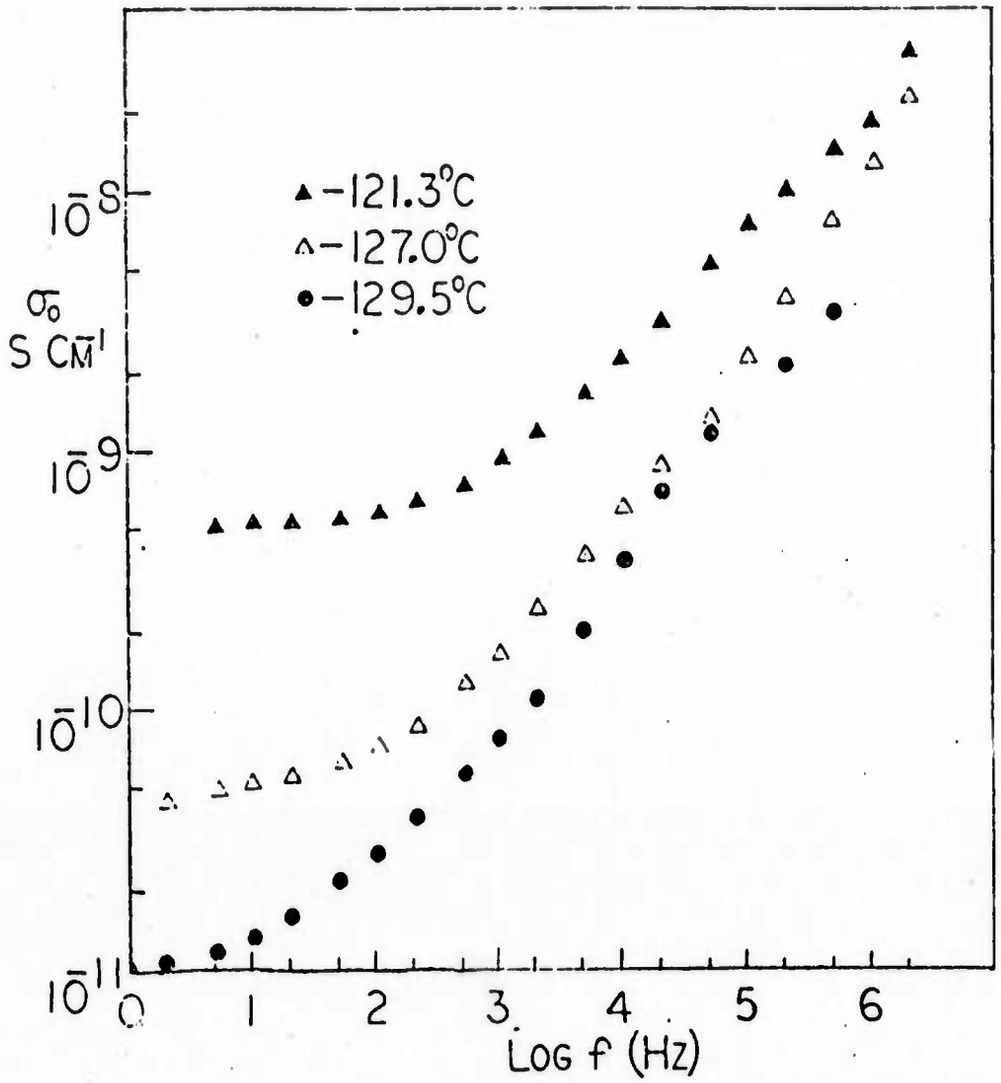

Figure 16

Specific Conductivity Frequency Dependences

for $H_2ZnCl_4.10H_2O$

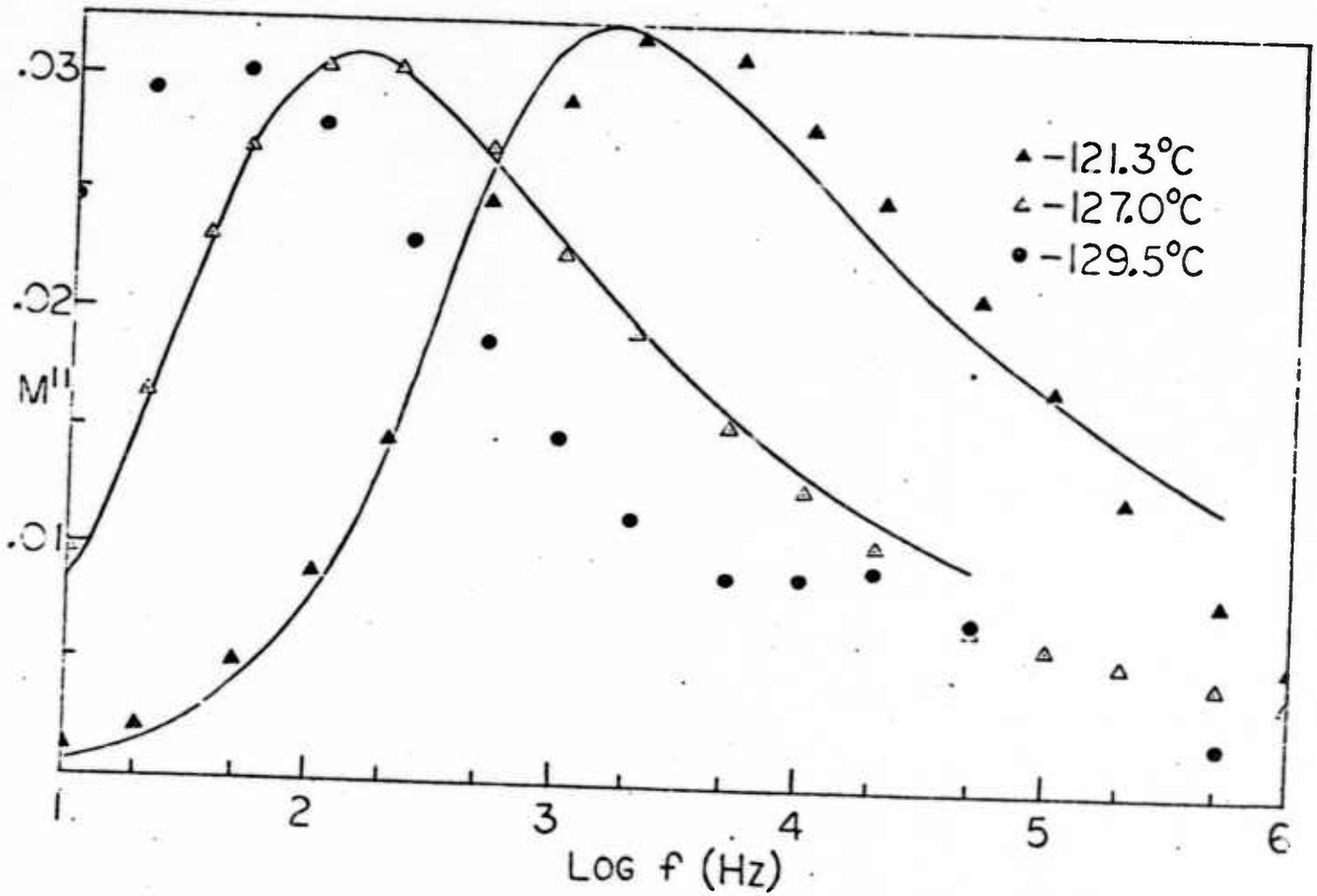

Figure 17

Cole-Davidson Fits to the Frequency of Imaginary Component of Dielectric Modulus for $H_2ZnCl_4 \cdot 10H_2O$

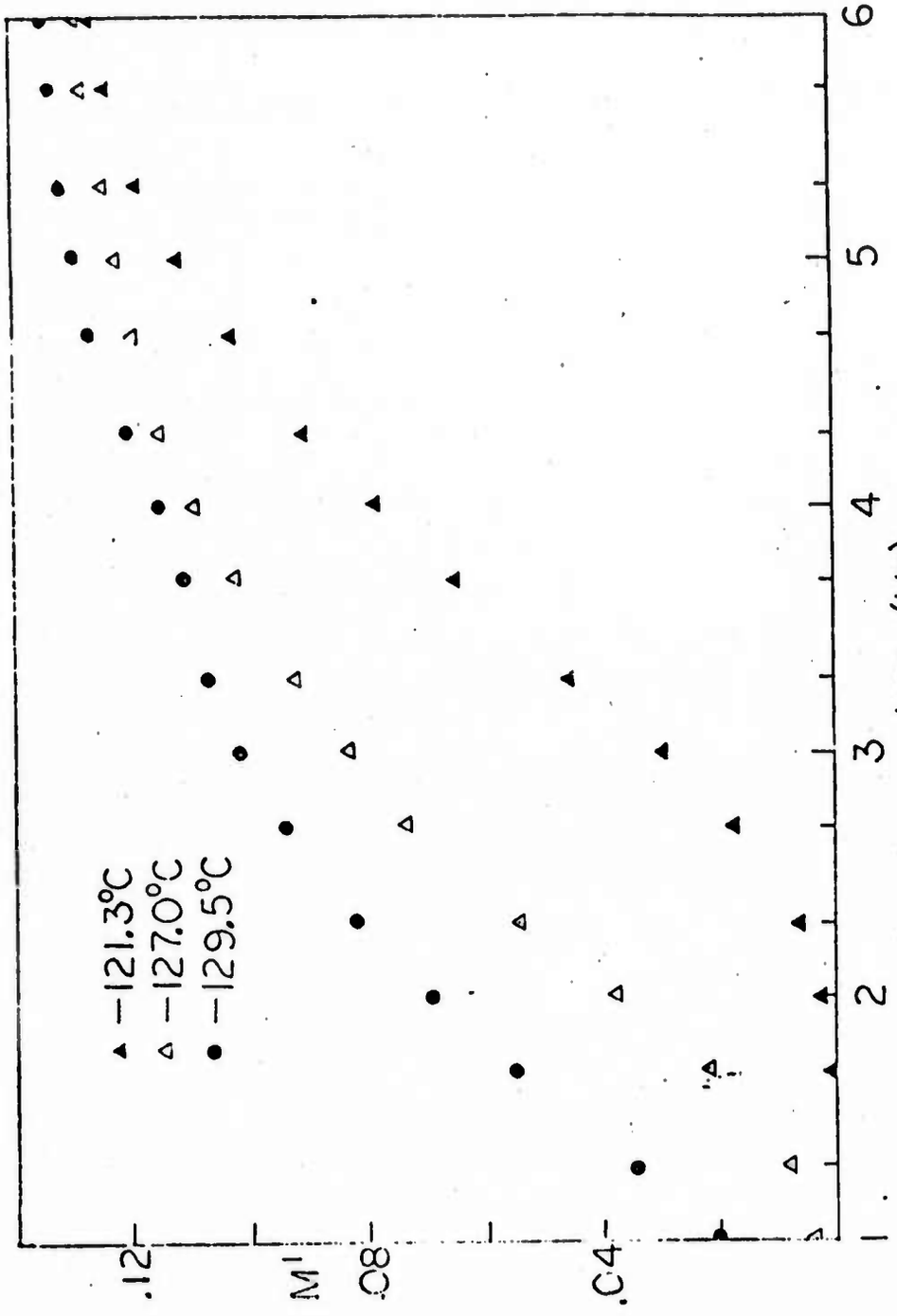

Figure 18

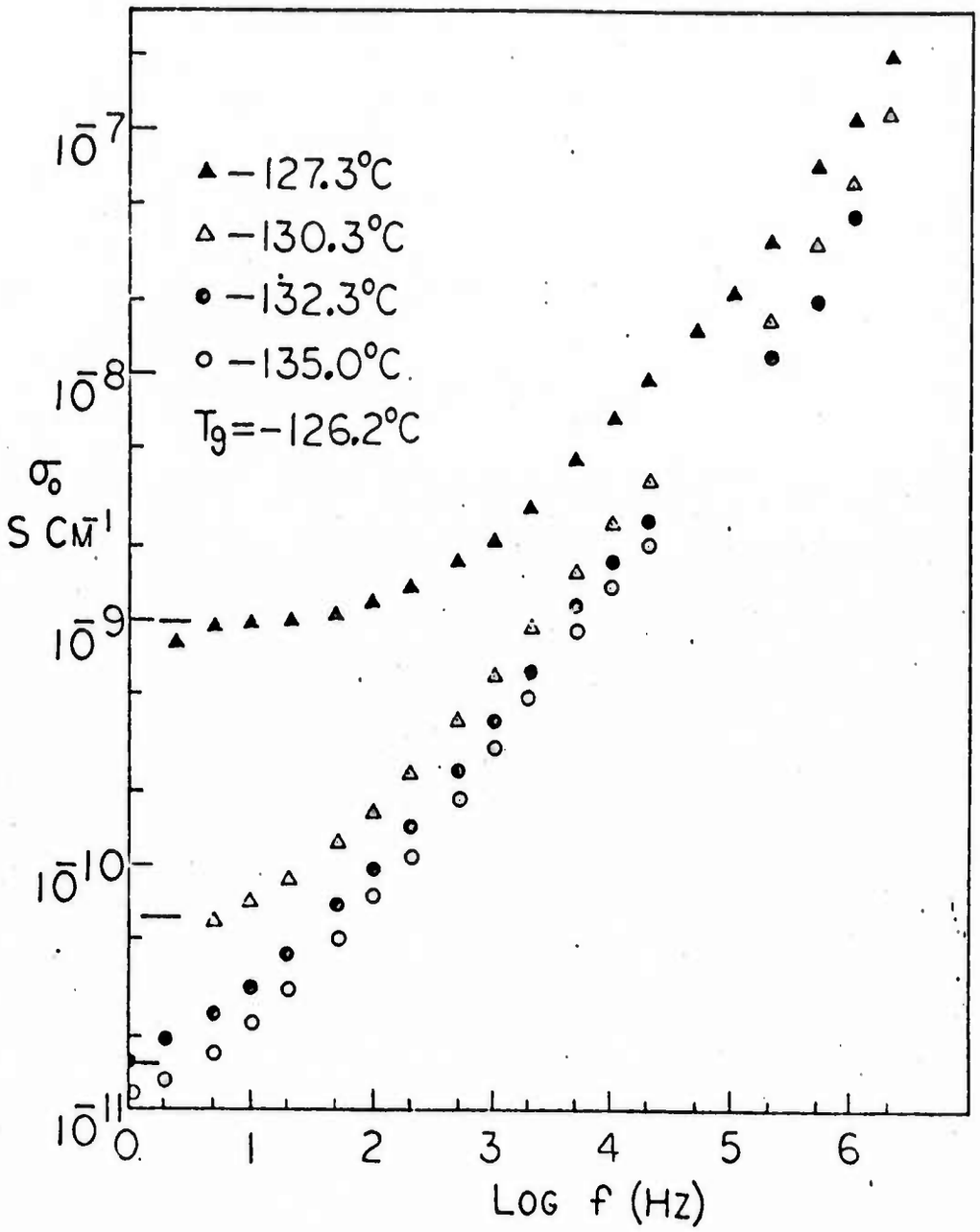

Figure 19

Frequency Dependences of Specific Conductivity for $H_2ZnCl_4.12H_2O$

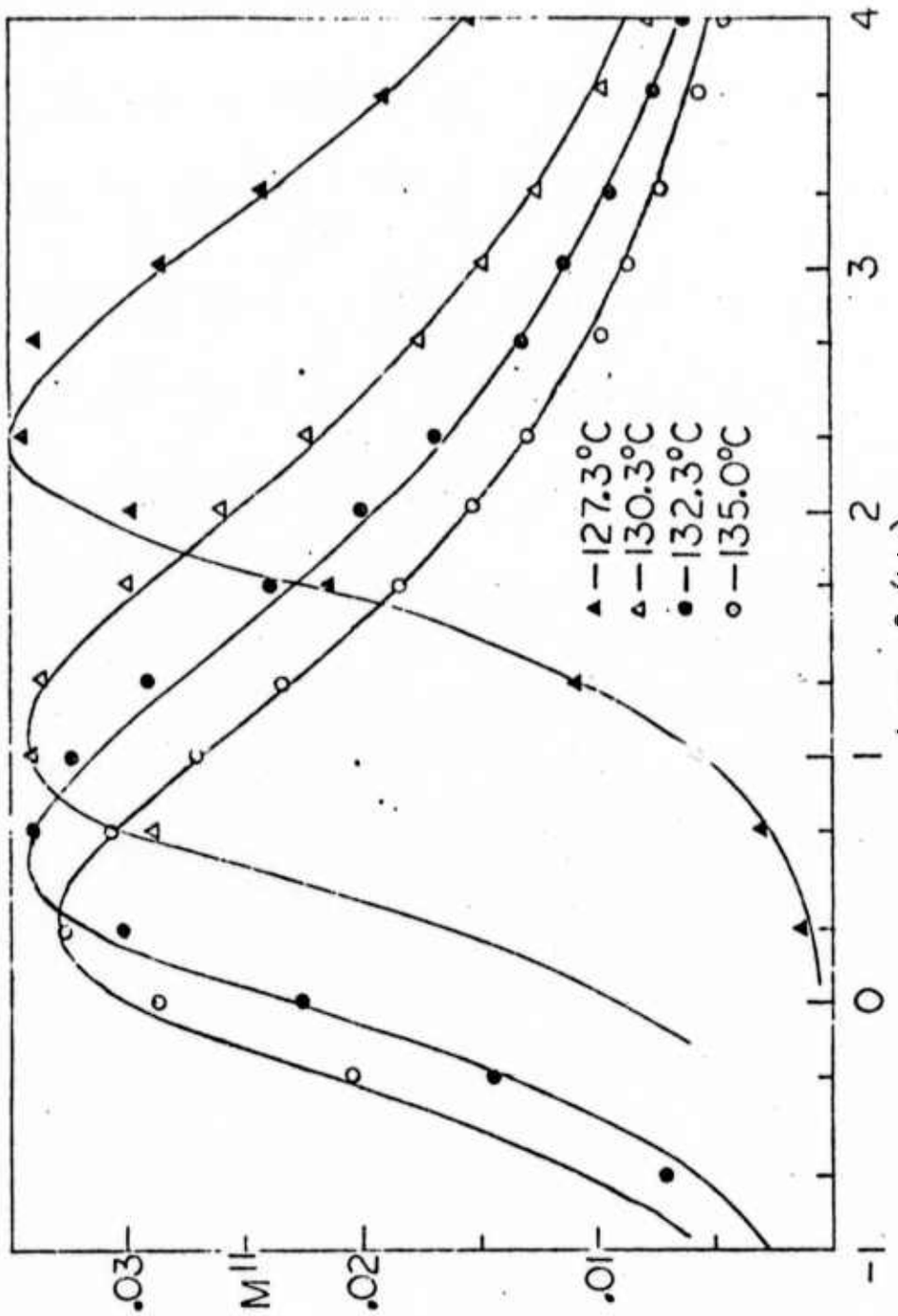

Figure 20

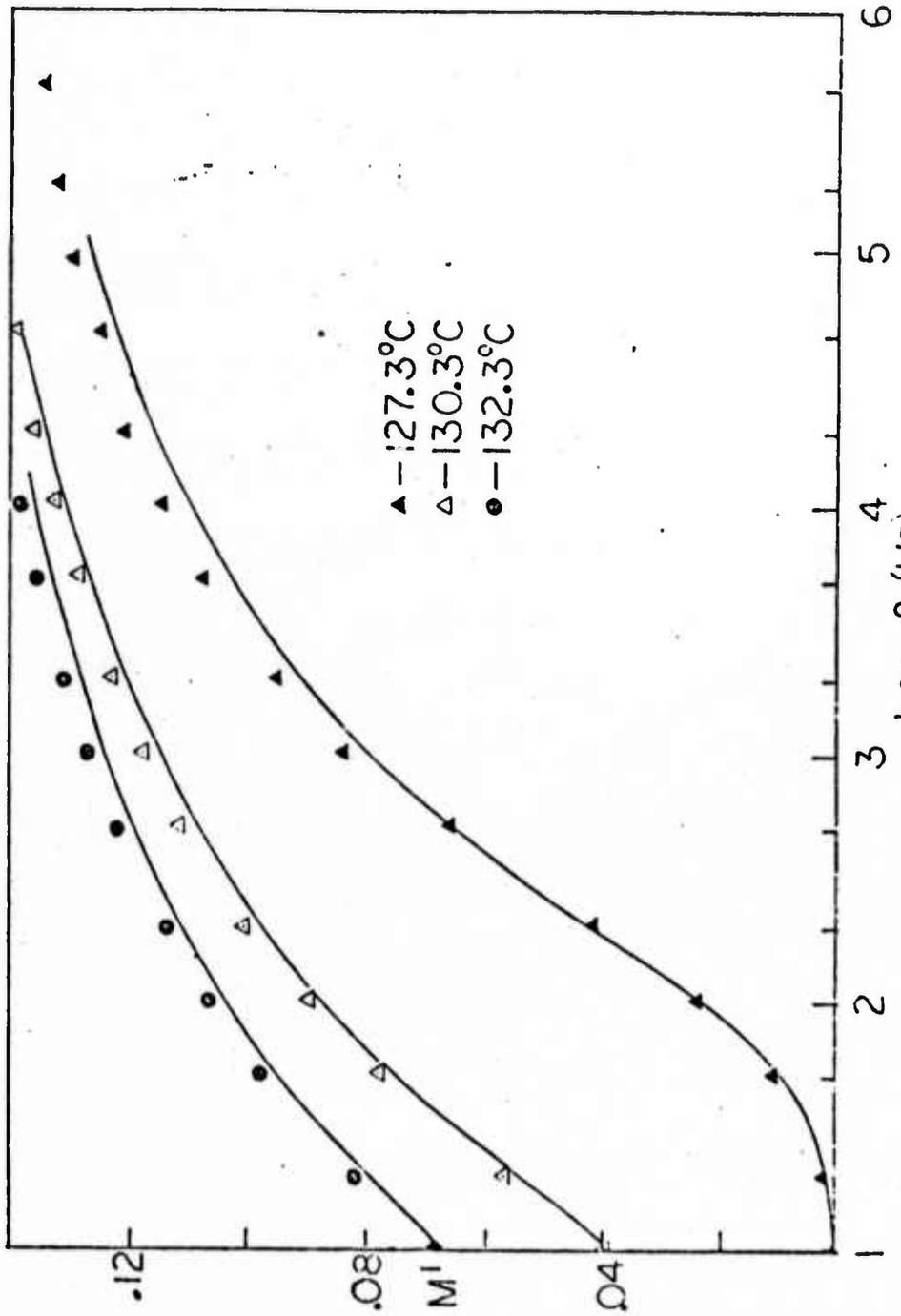

Figure 21

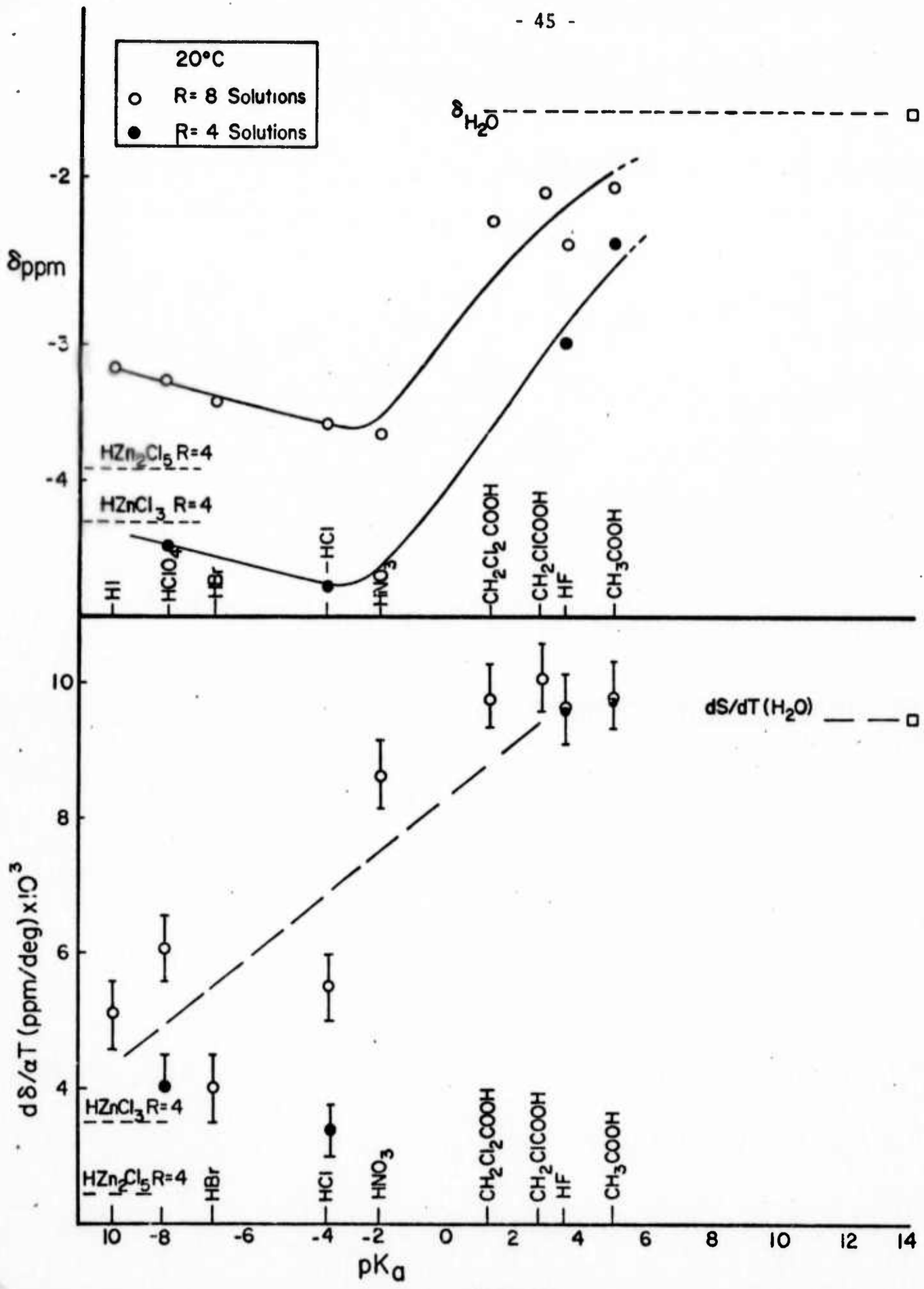
20°C
R= 8 Solutions
R= 4 Solutions
δ_{H_2O}
δppm
-2
-3
-4
HZn_2Cl_5 R=4
$HZnCl_3$ R=4
HI
$HClO_4$
HBr
HCl
HNO_3
CH_2Cl_2COOH
$CH_2ClCOOH$
HF
CH_3COOH
dS/dT (H_2O)
10
8
6
4
$d\delta/\alpha T$ (ppm/deg) x10^3
$HZnCl_3$ R=4
HZn_2Cl_5 R=4
10 -8 -6 -4 -2 0 2 4 6 8 10 12 14
pKa

Fig. 22

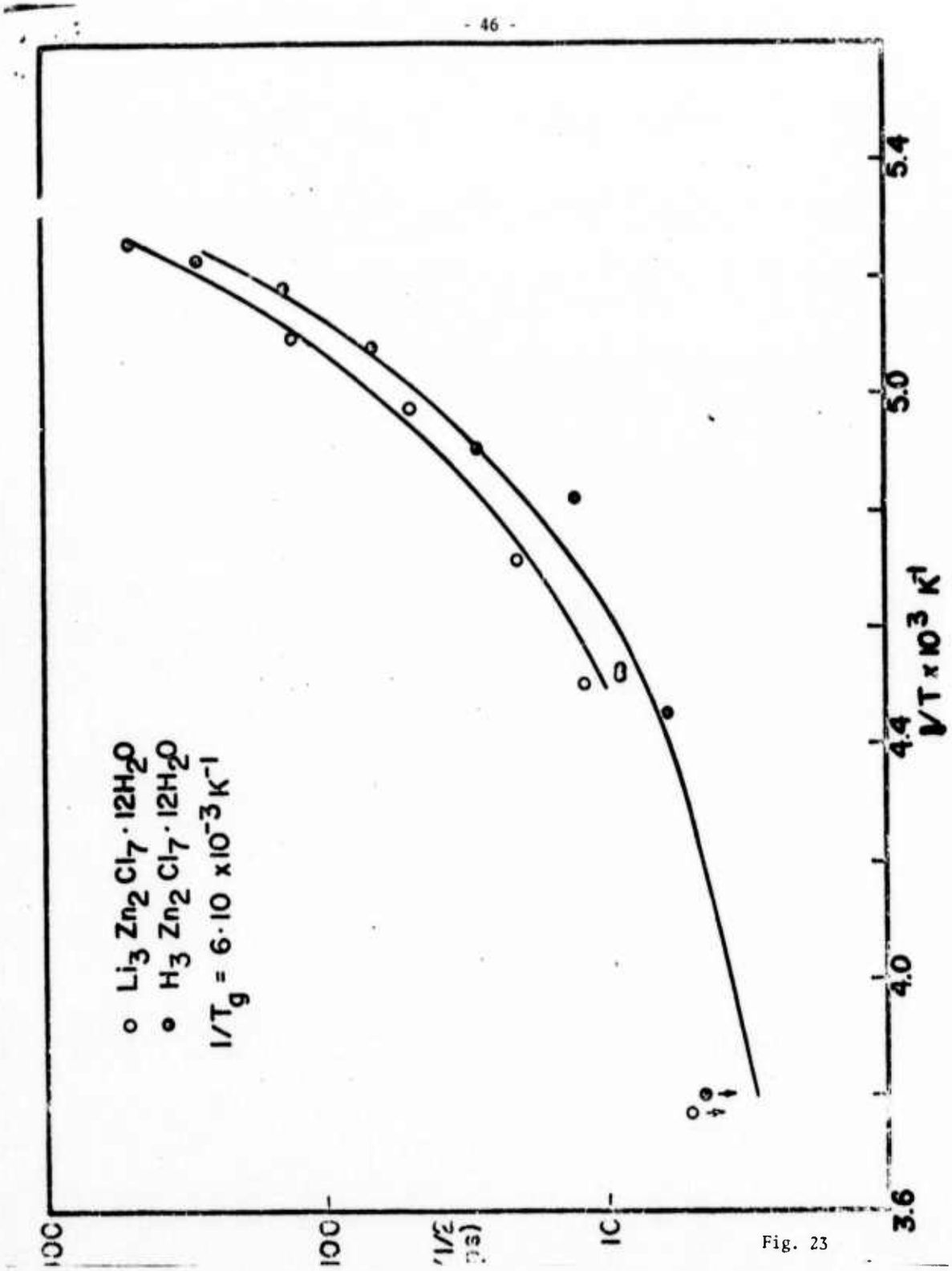
o $Li_3 Zn_2 Cl_7 \cdot 12H_2O$
• $H_3 Zn_2 Cl_7 \cdot 12H_2O$
$1/T_g = 6 \cdot 10 \times 10^{-3} K^{-1}$
$1/T \times 10^3 K^{-1}$
5.4
5.0
4.4
4.0
3.6
100
10

Fig. 23

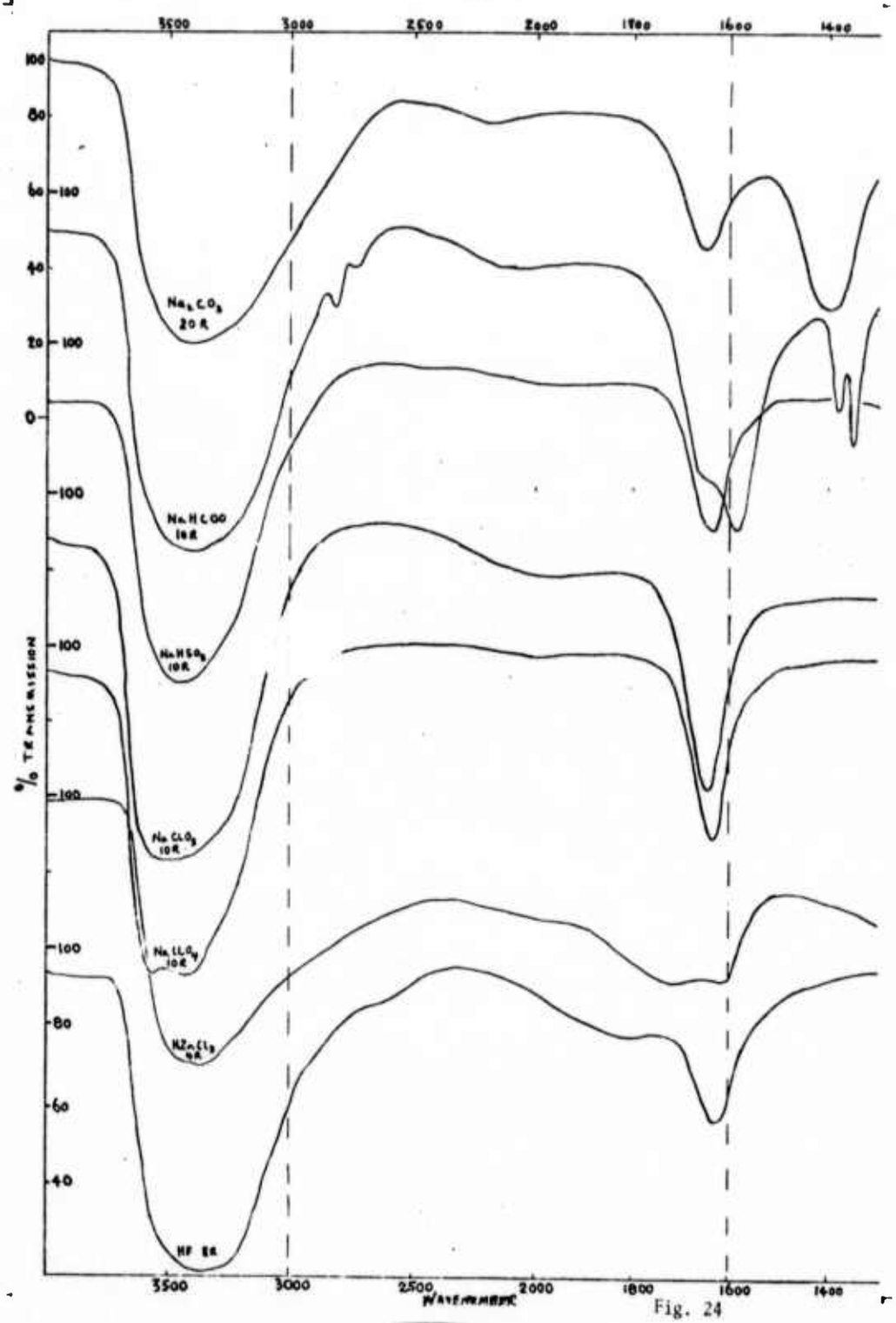
3500
3000
2500
2000
1800
1600
1400
100
80
60
40
20
0
% TRANSMISSION
Na2CO3 20R
NaHCO3 10R
NaHSO3 10R
NaClO3 10R
NaClO2 10R
HZnCl3 9R
HF 8R
WAVENUMBER

Fig. 24

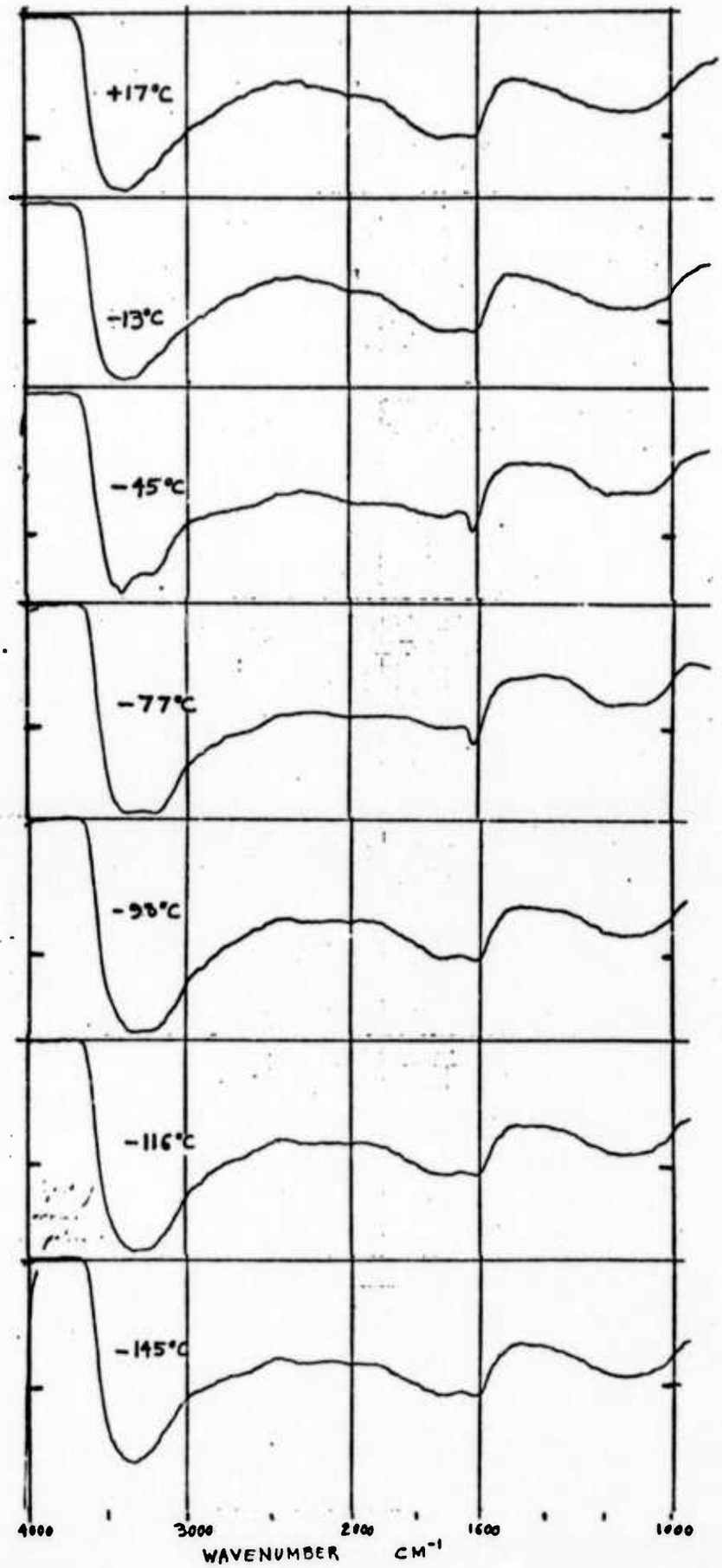
+17°C
-13°C
-45°C
-77°C
-98°C
-116°C
-145°C
4000
3000
2000
1600
1000
WAVENUMBER CM⁻¹

Fig. 25

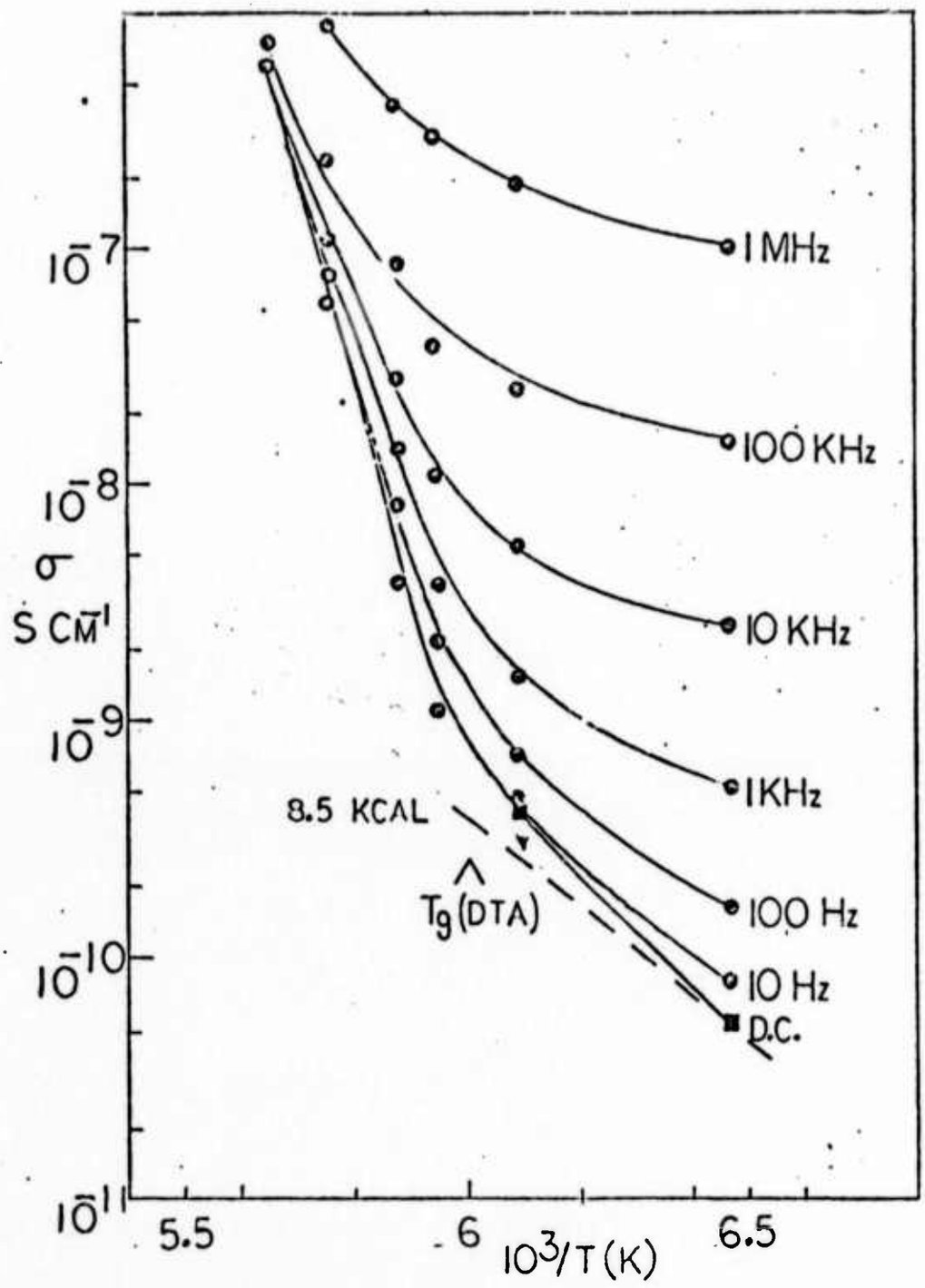

Fig. 26 Temperature dependences of conductivity for $HZnCl_3 \cdot 4H_2O$.

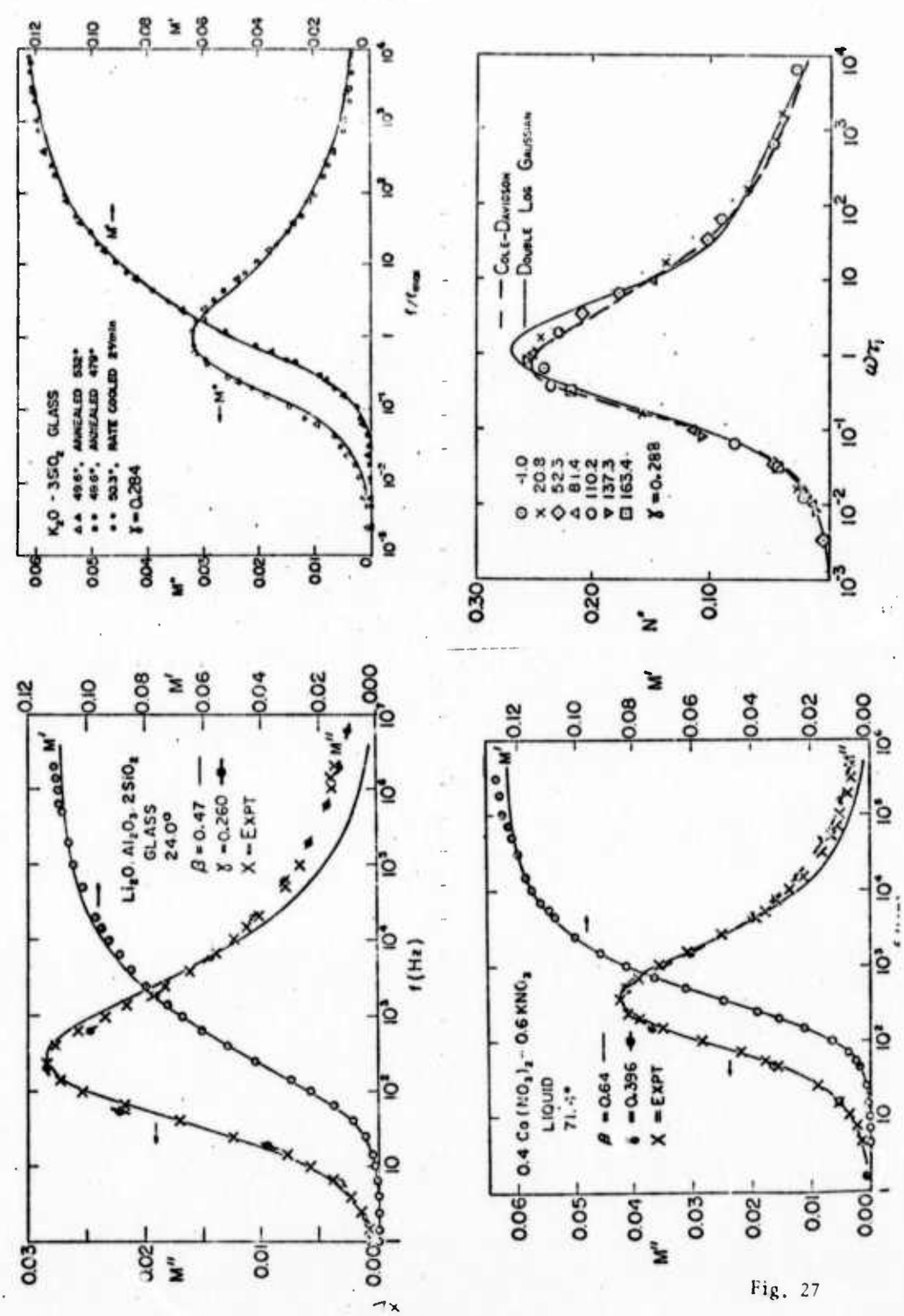

Fig. 27 Comparison of Cole-Davidson fits with Williams-Watts and Double log Gaussian fits, to literature data.